Ocean Engineering 172 (2019) 257–285

Contents lists available at ScienceDirect

Ocean Engineering

journal homepage: www.elsevier.com/locate/oceaneng

Review

A review on the modeling, materials, and actuators of aquatic unmanned vehicles

R. Salazar, A. Campos, V. Fuentes, A. Abdelkefi*

Department of Mechanical and Aerospace Engineering, New Mexico State University, Las Cruces, NM, 88003, USA

ABSTRACT

Aquatic robotics is making a critical transition to adapt and inspire more efficient systems from nature. The result is the abandonment of inefficient propeller-based locomotion for a biological locomotion type suitable for the specific mission. Bioinspired aquatic unmanned vehicles (AUVs) could be exploited in a diverse range of missions depending on the design and its capabilities. Removing the human pilot and creating an animal-based AUV means that more hazardous aquatic environments can be studied with reduced repercussions. There is a diverse range of biological locomotion's to choose from when developing a bioinspired AUV. The respective animals that exhibit a specific swimming mode give a range of criteria to follow make the system more capable of swimming. In this review, how previous AUV developers determined the kinematic, physical, and hydrodynamic modeling of these systems are consolidated and discussed. All types of developed actuators are reviewed, organized, and explained based on their materials and motion capabilities. The electronic components of these systems are outlined to give an idea of how these bioinspired AUVs are constructed. Then, it is discussed what makes these systems bioinspired and biomimetic, and the trends of these designs. Limitations and future recommendations on possible improvements for these systems are offered and deeply discussed.

1. Introduction

Robotic systems are being adapted to perform complex missions in aqueous environments (Blindberg, 2001; Colgate and Lynch, 2004; Habib, 2013; Wettergreen et al., 1998; Raj and Thakur, 2016; Murphy and Haroutunian, 2011). Aquatic unmanned vehicles (AUVs), alternatively referred to as unmanned underwater vehicles (UUVs), are receiving growing interest because of their potential to replace current aquatic tethered systems (Colgate and Lynch, 2004; Murphy and Haroutunian, 2011). Currently, aquatic robots are inefficient at moving because of their shape, use of propellers for thrust, and tethered control (Blindberg, 2001; Murphy and Haroutunian, 2011). Interest into the adaptation of biological motion creates robots which are capable at swimming like fish. These robots can perform routine swimming missions that would be considered hostile for hominid and outdated robotic investigations (Raj and Thakur, 2016; Scaradozzi et al., 2017a; Yen and Azwadi, 2015; Cruz et al., 1999). Clarification into the development of previous AUVs is needed to gain a better understanding so more optimized unmanned systems can be designed in the future.

AUVs can be applied in a range of missions for both civilian and military purposes. Missions include environmental surveying, oil spill monitoring, internal pipe inspection, erosion monitoring, observation of animal species, beach safety, espionage, anti-espionage, and border patrol (Blindberg, 2001; Najem et al., 2012; Tan, 2011; Lin et al., 2013; Diazdelcastillo et al., 2017; Lin et al., 2016). Each mission requires a specific capability which means designs must adapt to meet the increasing range of possible missions (Murphy and Haroutunian, 2011). With the potential for swarming based missions, AUVs could be exploited in collaborative missions that cover more space locations (Munasinghe et al., 2017). Currently, aquatic systems consider a rigid, boxlike or torpedo structure equipped with propellers and are controlled through use of a tether (Blindberg, 2001). However, these systems have difficulty maneuvering in close quarter environments and are inefficient in comparison with fish (Habib, 2013; Murphy and Haroutunian, 2011). The tether is cumbersome and makes it hard to maneuver as it has potential for getting snagged on obstacles, which can result in the failure of the mission. This causes the need for more natural and free moving systems that can complete a complex mission. Some systems have been equipped with non-propeller based thrust, a positive step forward (Guizzo, 2008; Rico et al., 2017). The new AUVs have been designed using actuation mechanism, materials, sensors, and batteries that condone bioinsipiration and biomimicry.

To express differences between animals and AUVs, work done by Murphy et al. (Murphy and Haroutunian, 2011) explains the capabilities of biological and mechanical systems through a comparative investigation of variables like speed, depth, turning capabilities, endurance, and cost of transport. In Fig. 1(a) and (b), examples of the differences between AUVs and biological animals are presented. Animals express better turning, endurance, and speed than robotic systems. In Fig. 1(b), circle size is a cost of transport function taking into account

* Corresponding author.
E-mail address: abdu@nmsu.edu (A. Abdelkefi).

https://doi.org/10.1016/j.oceaneng.2018.11.047
Received 23 July 2018; Received in revised form 4 October 2018; Accepted 25 November 2018

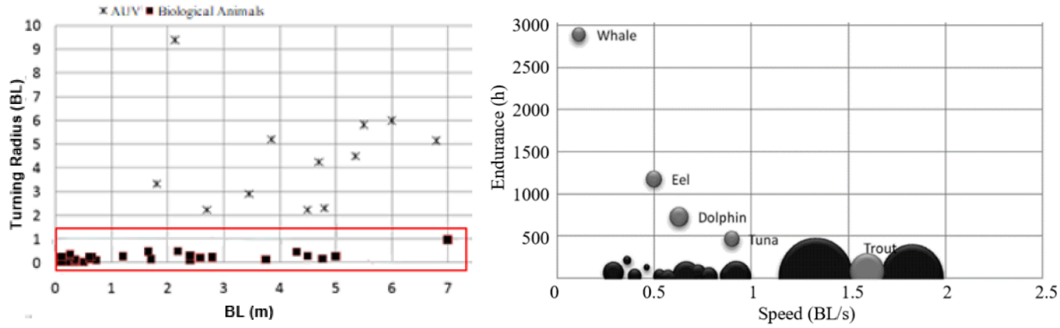

(a) (b)

Fig. 1. (a) Turning capabilities based on length, boxes enclosed in red rectangle are the biological animals while the crosses are AUVs. (b) The endurance versus speed is shown for biological animals (shown in light grey circles) and AUVs (shown in black circles) (Murphy and Haroutunian, 2011). BL stands for body length of the respective system.

the energy expended to swim per body mass. The larger biological animals require less energy to swim and have much higher endurance.

Studies have been conducted where the focus has been placed on analyses and validations of AUVs that are capable of autonomous swimming (Colgate and Lynch, 2004; Raj and Thakur, 2016; Yen and Azwadi, 2015; Cen and Erturk, 2013; Neveln et al., 2013; Webb and Weihs, 2015; Shen et al., 2015). These investigations offer insight into the methods performed to create the most optimal systems. The sections that are determined to be the most important and are considered in this review are as follows: (2) biological terminology, (3) kinematic and dynamic modeling, (4) hydrodynamic analyses, (5) actuators, (6) materials, (7) sensors, (8) batteries, (9) discussion and future recommendations, and (10) conclusions. This review consolidates and organizes these topics in a manner that will allow for more optimized AUVs to be created. Understanding the following topics in detail allows for the optimal methods to be discussed and used in the future.

2. Biological terminology

This review describes these categories of locomotion which pertain to Fin Oscillation, Fin Undulation, and Jet Propulsion species, as shown in Fig. 2. If more knowledge is required on this categorization and respective biological and robotic systems, the readers are referred to a recent review work by Salazar et al. (Salazar et al., 2018a). The key terms that need to be recognized for the biological animals are the body characteristics and structures needed for thrust and control by the respective. The physical characteristics are considered important for AUV adaptation and optimization.

The physical terminology that is defined for all animals is shown in Fig. 3. The forces expressed by the system are depicted in Fig. 3(a). While Fig. 3(b) and (c) represent the three directions the body can move during swimming.

Caudal fin animals utilize an oscillating body flexion to actuate the tail which is known as body caudal fin (BCF) locomotion (Scaradozzi et al., 2017a; Sfakiotakis et al., 1999; Lauder, 2015; Zhou et al., 2017). Utilization of a caudal fin allows species to achieve fast speed (Sfakiotakis et al., 1999). The animals in this class generally bony and

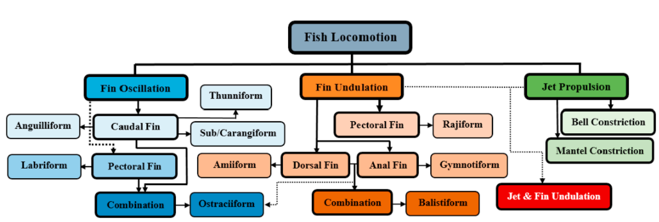

Fig. 2. Considered classification for individual animal/AUV locomotion (Salazar et al., 2018a).

have a spinal structure to support the body. Fin undulation species excite individual rib structures in the fin to cause undulations along the fin length. Certain species in the Rajiform, Gymnotiform, and Balistiform category are capable of forward and reverse swimming directions depending on the wave direction. This class is a mixture of bony and cartilaginous animals, body structures vary greatly depending on the species selected. Jet propulsion animals contract their bodies to forcibly expel water from an internal cavity. The body of these animals lack rigid structure so complex musculature gives the body motion and support. There are many combinations between these three main categories, each with their own unique method of locomotion.

3. Kinematic and dynamic modeling

To create models for the characteristics of biological systems, various methods are used. It can be found that there are a multitude of swimming styles expressed by aquatic animals. This includes, but is not limited to, animals that use caudal fins, pectoral fins, dorsal or anal fins. These fins can either perform oscillatory or undulatory motions to produce thrust. For Jet Propulsion, animals compress water by clenching a mantel or bell. These different swimming styles require specific motions to generate the required thrust. For the AUVs, these models give the required motion for surfaces so thrust can be optimized.

3.1. Kinematic modeling

Kinematic modeling is obtained through the observation of living specimens. These living specimens give the motion and velocity characteristics for the body. Moreover, this methodology helps to obtain shape of propulsion surfaces and body. Distinct criteria of the individual species can then be replicated when designing an actuation mechanism. Methods for biological observation include body and fin marker tracking using cameras in a controlled environment like a water channel or static fluid tank.

3.1.1. Fin Oscillation kinematic modeling

Spinal flexion modeling is considered for animals that utilize a caudal fin, shown in Fig. 4. MPF motion has been tracked for fishes in the Labriform and Ostraciiform subcategories, where models for these cases are based on the fin edge, shown in Fig. 5.

Biological motion is created for species through the complex retraction and relaxation of the muscles along body. Fig. 4(b) is a representation of one complete cycle for a Carangiform fish. It can be noted that muscle activation initiates behind the head to the tail peduncle. The more flexible Anguilliform species express more alterations between the lengthening and shorting of their lateral muscles expressing more than one wave period (Gillis, 1996; Videler et al., 2001). MPF

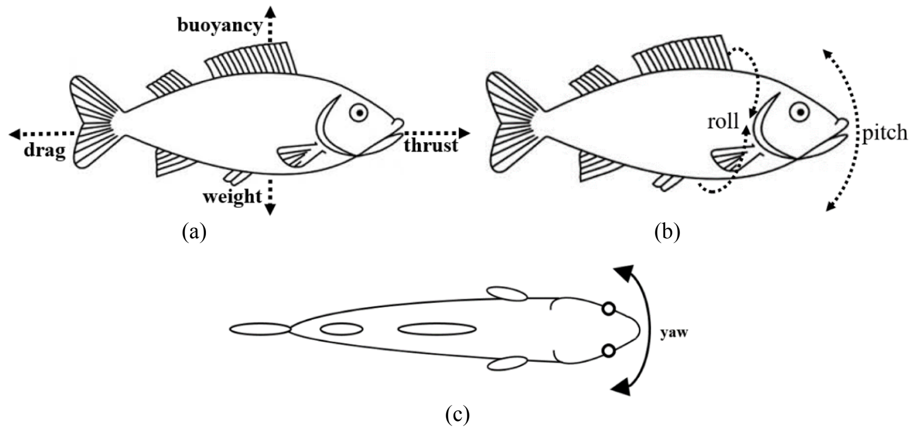

Fig. 3. Terminology for (a) the free body diagram a fish, and (b) the directional change with respect to pitch and roll, (c) and directional change respect to yaw (Salazar et al., 2018a).

fishes do not require the large lateral muscle activation as these fins have more localized muscle around the fin (Westneat, 1996).

Fig. 6 is a marker spinal curvature model which gives one phase in propulsive cycle. By determining the motion of the spine, the most basic motion can be extracted for each type of caudal fin motion. For Anguilliform, the spinal curvature is more complex as the body performs larger wave amplitudes and also have multiple periods over the body length. The Subcarangiform and Carangiform have similar body undulation, but the Subcarangiform has greater head amplitude to initiate the body undulation (Sfakiotakis et al., 1999). Thunniform fishes have the smallest head amplitudes while the body undulation is restricted to the peduncle.

These types of oscillations are modeled using a combination of different sinusoidal curves with varying amplitudes (Colgate and Lynch, 2004; Scaradozzi et al., 2017a; Yu et al., 2016a; Cui et al., 2017; Clapham and Hu, 2014; Liu et al., 2005; Bergmann and Lollo, 2011; Khalid et al., 2016). These models are usually constructed using a quadratic polynomial function as an envelope for a sinusoidal wave, as shown in Eq. (1):

$$y(x, t) = (a_0 + a_1 \cdot x + a_2 \cdot x^2) \cdot \sin(\omega t - kx) \quad (1)$$

The polynomial function expresses the amplitude envelope of the lateral motion of the spine as a function of space. The wave number (k) of the body undulations that corresponds to the wave length and angular frequency are considered in the sinusoidal term (Borazjani and Sotiropoulos, 2010). The terms a_0, a_1, and a_2 are coefficients of the amplitude envelope.

The tracking for MPF swimmers requires an understanding of the fin motion. Due to fin rotation during power and recovery stroke, multiple markers are used to track both the leading and trailing edges, respectively, as shown in Fig. 5(a). Labriforms are capable of different types of propulsive fin stroke performing flapping or rowing motions, as presented in Fig. 5(b–d). Shown for the flapping motion, the power stroke occurs on the downstroke, while the power stroke for the rowing motion occurs when the fin is pulled back. Recovery during the rowing motion is much more drastic as the fin transitions to a flat position to the fluid flow to minimize drag. Flapping is carried out by the leading edge plunging the greatest distance in the y-direction compared to the trailing edge, as shown in Fig. 5(b) and (c) (Walker and Westneat, 1997; Walker and Westneat, 2002). The angle of the flapping stroke is along vertical axis perpendicular to the body where the rowing stroke is more of a lateral plane to the body (Walker and Westneat, 2002). Shown in Fig. 5(e), the fin tip displacement for the rowing motion can occur at a certain angle of attack depending on the swimming speed and control the animal desires. These motions are more difficult to model as swimming gait transitions for different speeds. Numerical methods like those considered by Shoele et al. (Shoele and Zhu, 2010) have shown

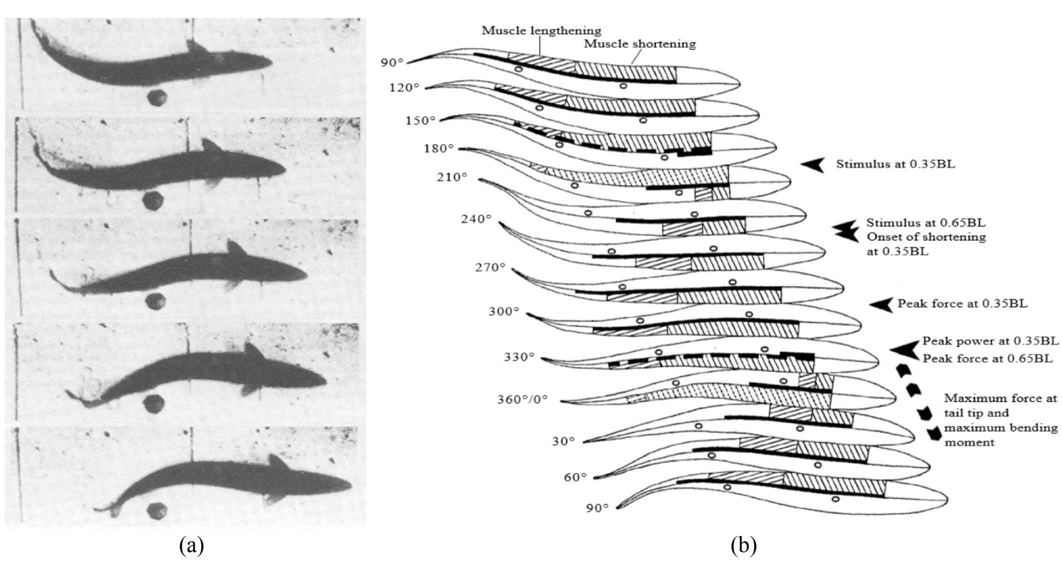

Fig. 4. Biological Carangiform (a) motion caught on video with various reference markers (Wardle and Videler, 1980) and (b) musculature function during one oscillatory cycle (Altringham et al., 1993).

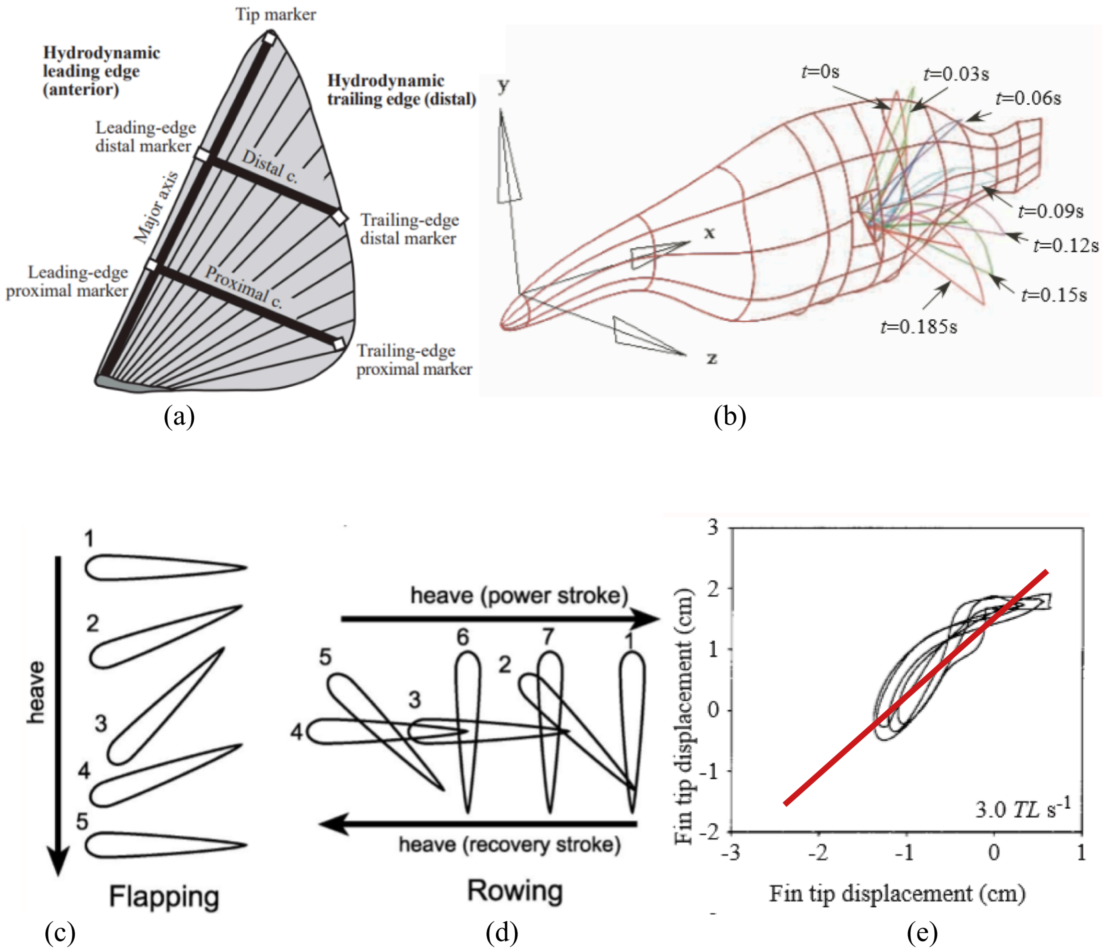

Fig. 5. (a) Marker trackers for the pectoral fin motion (Walker and Westneat, 1997), (b) model for Labriform pectoral flapping fin motion (Ramamurti et al., 2002), (c) rudimentary Labriform flapping, (d) rowing motions obtained from (Walker and Westneat, 2002), and a model of Ostraciiform pectoral fin tip displacement during a set swimming speed experiment, modified from (Hove et al., 2001) as the red line shows the angle of attack for rowing stroke.

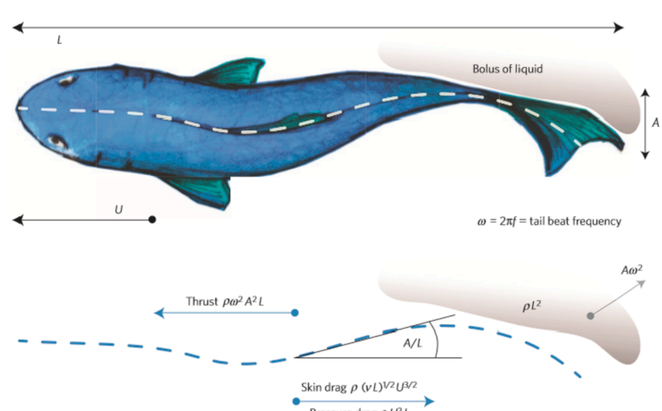

Fig. 6. Example of a biological caudal fin fish and the resulting spinal curvature model (Gazzola et al., 2014). Schematic shows the area displaced by the tail flexion, fish velocity (U), thrust is shown to be in the direction of velocity, skin and pressure drag are in the opposite direction of velocity, frequency (ω), and tail amplitude of oscillation (A).

that it is possible to model some of the swimming motions of a Labriform. Flapping is mostly used for slower speed swimming while a rowing motion is used for higher speeds (Walker and Westneat, 2002; Sitorus et al., 2009). However, once the muscles for pectoral locomotion are exhausted, these animals can utilize a BCF locomotion to maintain speed (Davison, 1988). There are a few AUVs that consider the caudal fin in the Labriform design, higher emphasis is put on the pectoral motion.

Ostraciiforms use the pectoral, dorsal/anal, and sometimes the caudal fin depending on the species. The pectoral fins and single dorsal and anal fin are primarily used at lower speeds, while the caudal fin can be used at higher speeds (Wang et al., 2013). Same as the Labriform, the higher the speed the more lateral the flapping motion (Hove et al., 2001; Wang et al., 2014). The dorsal and anal fins should be synonymous with a flapping motion as the leading edge of the fin performs the greatest plunging amplitude. The dorsal and anal fins are used for increased stability as they correct yaw and roll for these fishes.

3.1.2. Fin undulation kinematic modeling

Animals in this class use a flexible fin membrane as propulsive surfaces. The support structures of these fins are often ribs whose flexibility depends on the species. Traveling undulatory waves of these fins need to be studied as they create thrust to move the body forward, and stabilize the animal while it swims. Wave amplitude and frequency are unique for each species.

Considering the Fin Undulation category, Sfakiotakis et al. (Sfakiotakis et al., 1999) described the translational wave that these animals initiate causes perpendicular and parallel force to the fin base. These forces are what give these animals their unique stability and maneuvering capabilities (Lauder, 2015). The Rajiform category contains animals like the Cownose Ray and Manta Ray, shown in Fig. 7(a). The leading fin edge performs a greater plunging amplitude relative to the trailing edge while the surface of the fin can exhibit a traveling

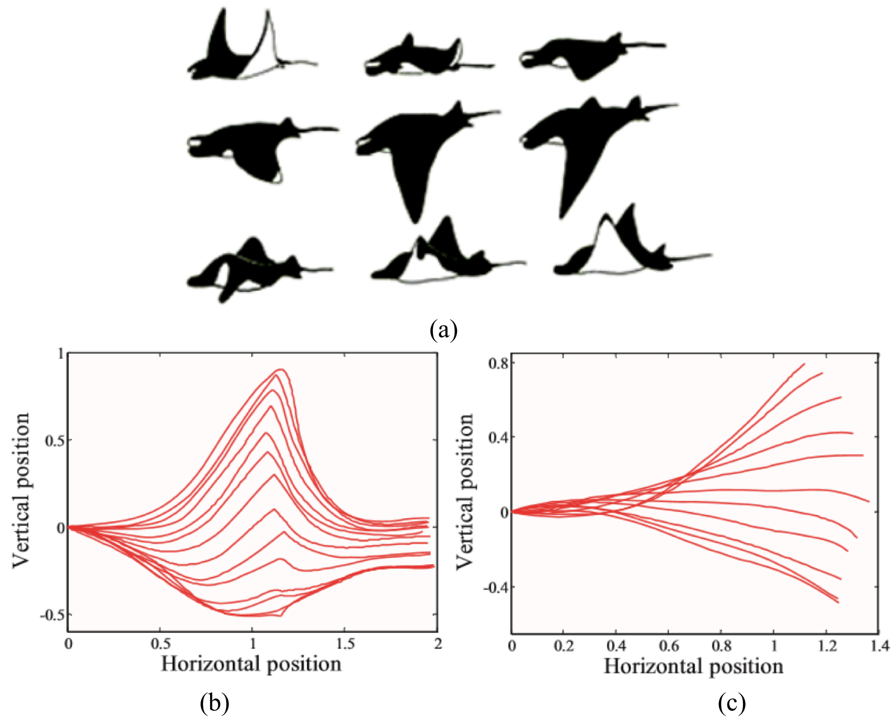

Fig. 7. (a) An illustration for the swimming motion for a Manta Ray, obtained from (Wang et al., 2009). Biological motion of Cownose Ray (Rajiform) obtained from video for one downstroke: (b) a side view of the downstroke motion, and (c) the leading edge of that same motion (Zheng et al., 2010).

wave. Where the fin motion appears as oscillatory, but the flexibility of the fin over its span makes it undulatory. The flapping motion of the Manta Ray is similar to the Labriform flapping motion, but the larger cartilaginous pectoral fin is for sure more flexible. Videography helped to discretize the specific flapping motion for a Cownose Ray, as shown in Fig. 7(b) and (c) (Zheng et al., 2010).

The Stingray, also a Rajiform, exhibits a different undulation wave compared to the Cownose Ray as it uses isolated wave propagations along the fin span to swim. The multiple wave propagations along the fin is shown in Fig. 8(a) and (b). Work by Blevins et al. (Blevins and Lauder, 2012), Bottom et al. (Bottom et al., 2016), and Daniel (Daniel, 1988) describe how to model the three degree of freedom wave propagation expressed by Rajiform species. The modeling of the fin curvature was done using marker lines with multiple points that are perpendicular to the spine, as presented in Fig. 8(c). These extremely flexible fins are capable of multi-directional wave propagation, waves can translate from front to back and *vice versa*. Each fin can behave independently of the other, each fin displaying its own wave direction, allowing these animals to make null speed turns.

For Amiiform and Gymnotiform, individual ribs and a flexible interstitial membrane make these fins extremely flexible, and allow multiple periods to be expressed by the fins (Xiong and Lauder, 2013; Sprinkle et al., 2017). Work by Hu et al. (Hu et al., 2009) and Youngerman et al. (Youngerman et al., 2014) are good examples of videography and modeling of Amiiform and Gymnotiform locomotion, as depicted in Fig. 9(a) and (b), respectively. Youngerman et al. (Sprinkle et al., 2017) described four different swimming styles for a Gymnotiform and the corresponding wave propagations used in forward, backward, vertical, and roll swimming. Each swimming style requires a specific wave propagation frequency, amplitude, and direction. Shown in Fig. 9(c), a traveling wave for forward swimming changing position over time is marked by the dashed line. Efforts by Hu et al. (Hu et al., 2009) model the ribbon fin kinematics of the Amiiform which is synonymous with the Gymnotiform. Flexibility of fin ribs and membrane is shown in Fig. 9(d).

3.1.3. *Jet propulsion kinematic modeling*

The Jet Propulsion category is unique in that the whole body is flexible. These animals do not have a rigid skeleton or rib structure; therefore, these creatures are entirely soft bodied. However, complex musculature structure allows these animals to contract and create thrust. For Jet Propulsion, the shape deformation is modeled to determine the volume displacement, as shown in Fig. 10.

The bell of the Jellyfish has been observed for the flexion curves

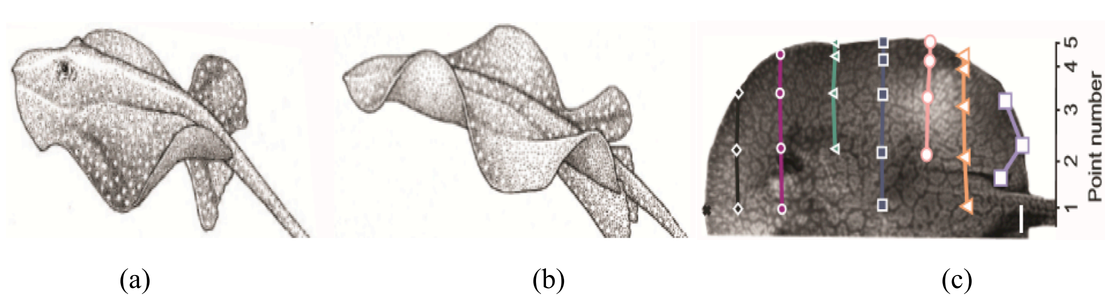

Fig. 8. Diagrams (a) and (b) are for the side view of a Stingray with two wave propagations along the fin length, and (c) is the marker array used for the wave modeling (Blevins and Lauder, 2012).

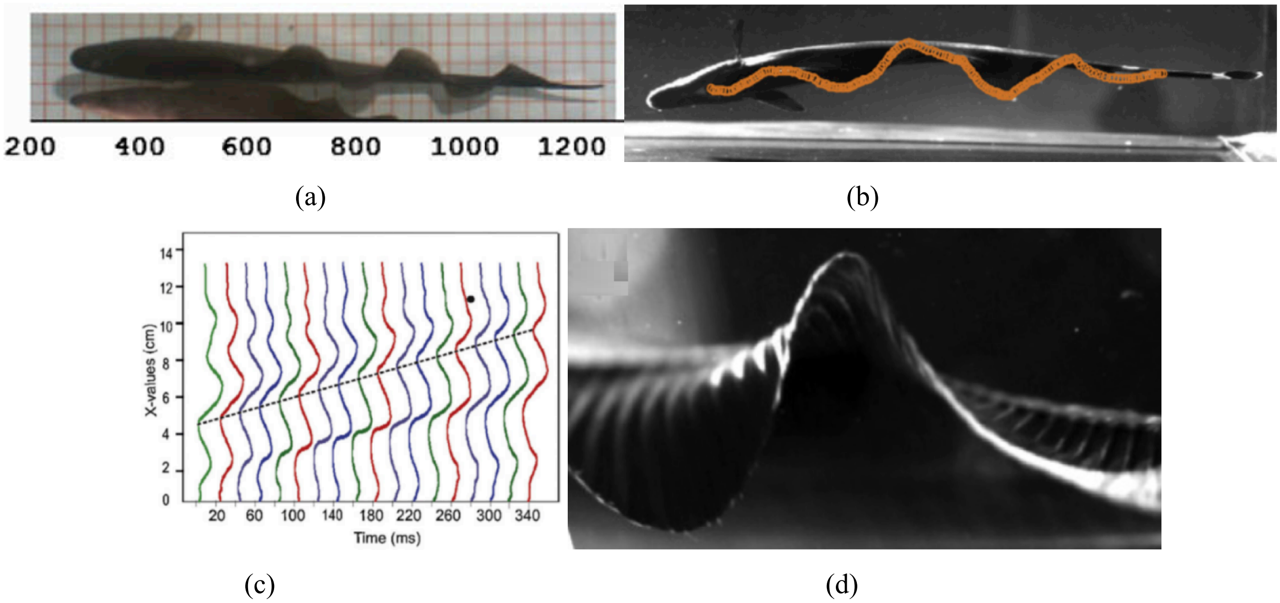

Fig. 9. (a) Still shot of African Aba Aba (Amiiform) (Hu et al., 2009), (b) the fin marker tracking for a Ghost Knifefish (Gymnotiform), (c) modeled wave propagation for forward swimming of the Ghost Knifefish, and (d) close up picture of the highly flexible fin (Youngerman et al., 2014).

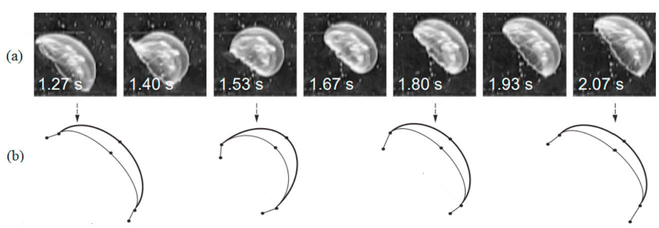

Fig. 10. One complete propulsive cycle for the Aurelia aurita Jellyfish (a) video frames, and (b) the corresponding kinematic model as obtained from (McHenry and Jed, 2003).

analyzed from the oblate and prolate shapes. Oblate Jellyfish are described by a flatter shape with a large bell radius. Prolate Jellyfish have more of a bullet shape where radii and body sizes are smaller than oblate Jellyfish. Jellyfish produce the bell motion through constriction of muscles in the subumbrella, allowing them to eject water out of the semi enclosed volume of their bell. As explained by McHenry and Jed (McHenry and Jed, 2003) and Dabiri et al. (Dabiri et al., 2005), Jellyfish's motion consists of continuous contraction and relaxation phases. Oblate jellyfish are known to generate thrust by paddle swimming, characterized by none symmetric bell constrictions. Prolate Jellyfish have symmetric bell constriction, often at a much higher frequency than the oblate. The Aurelia aurita exhibits both cases of the oblate and prolate swimming styles making them good candidates for observation. Fig. 10(b) allows for a clear observation of the contraction and relaxation phases created from the body markers in the videography experiments for Aurelia aurita Jellyfish as depicted in Fig. 10(a).

Other subsections of the Jet Propulsion classification are the mantel constriction and combination of Fin Undulation with mantel constriction. Mantel constriction is expressed solely by animals like the Octopus. This animal utilizes inhalation of water into a mantel cavity and forcibly expelling it from a siphon creating thrust. The combination class of mantel constriction and Fin Undulation pertains to animals that utilize the same mantel constriction as the Octopus, but also have undulatory fins capable for slow motion control. Biological species in this category are the Squid and Cuttlefish. Bartol et al. (Bartol et al., 2001) described the swimming behavior of the Squid (Lolliguncula brevis) by using video frames, as shown in Fig. 11(a) and (b). Mantel constriction is achieved by the contraction of three-directional muscle weave in the mantel (Johnson et al., 1972). The mantel can fill more than twenty-percent compared to the relaxed state, and can expel this water till the mantel is more than fifteen-percent smaller than the relaxed state (Johnson et al., 1972). The cycle of mantel constriction is shown in Fig. 11(c). Bortal et al. (Bartol et al., 2001) also described that the Squid uses its undulator fin in forward and backward swimming. Jet Propulsion is primarily utilized in backward swimming for fast escapes (Weymouth et al., 2015).

3.2. Physical modeling

The physical modeling of the system is done most often through a theoretical assumption of the hydrodynamic parameters that partake in the swimming motion, namely, thrust and drag. Parameters of interest for studies are the Reynolds (*Re*) and Strouhal (*St*) numbers, which are a function of the frequencies. Investigators like Cui et al. (Hove et al., 2001) define these parameters for Carangiform fish and result in the following equations:

$$Re = \frac{L^2}{T \cdot \upsilon} \tag{2}$$

where υ is the kinematic viscosity, $T = 1/f$ as T is the beating period, and L denotes the fish length. As for the Strouhal number, its expression is given in Eq. (4) where A_{max} represents the maximum tail amplitude of oscillation, and U is the speed of the fluid when the body is considered to be traveling at null speed (Cui et al., 2017; Tolkoff, 1999).

$$St = \frac{f \cdot A_{\max}}{U} \tag{3}$$

The lift and drag forces can be found through a simplified, numerical, or experimental analysis. If the pressure and shear stress distribution are known over a studied shape, then these forces can be found through Eqs. (5) and (6) as follows (Munson et al., 2013):

$$F_{Drag} = F_{D_{pressure}} + F_{D_{viscous}} = \oint P \cdot \cos\theta dA + \oint \tau_w \sin\theta dA \tag{4}$$

$$F_{Lift} = F_{L_{pressure}} + F_{L_{viscous}} = -\oint P \sin\theta dA + \oint \tau_w \cos\theta dA \tag{5}$$

These equations account for the effects of pressure differences and the viscous effects induced by the shape by integrating to get the total respective force in a coordinate direction (Munson et al., 2013). These

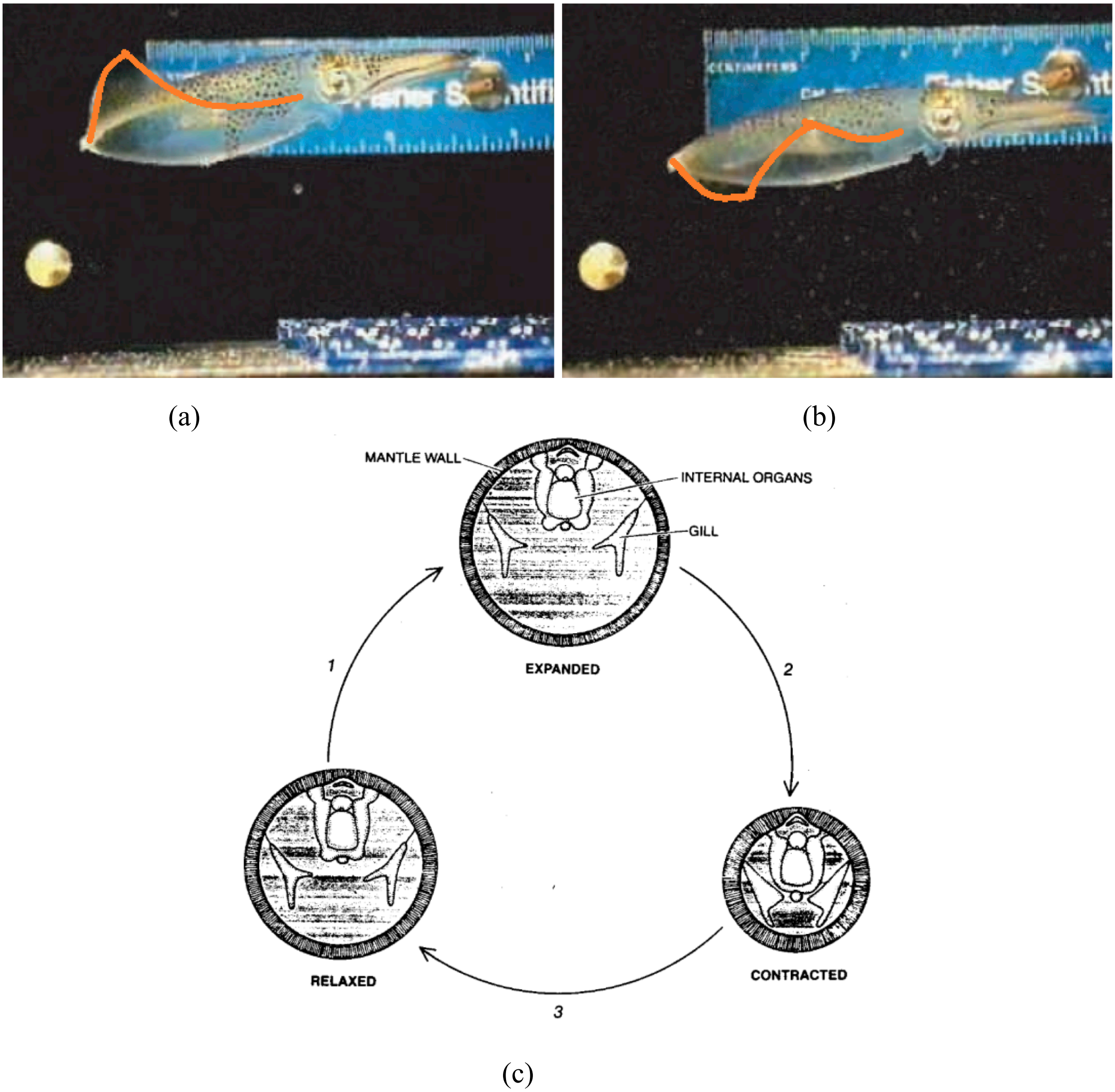

Fig. 11. (a) and (b) Video frames of the undulated fin swimming of a Squid, modified from (Bartol et al., 2001) to show the fin undulation observed, (c) the contraction of the mantel for the squid obtained from (Johnson et al., 1972).

terms are most commonly found for airfoils (Abbott and Doenhoff, 1959), but more detailed force approximations are being made for objects of complex shape (Batchelor, 2000; Vasudev et al., 2014). Here, the pressure (P) over the surface and the wall shear stress (τ_w) from the fluid moving past the surface (Abbott and Doenhoff, 1959). For assumed shapes, coefficients for lift and drag can be approximated using Eqs. (7) and (8) (Munson et al., 2013). For neutrally buoyant bodies, lift from fins can be important for depth and roll control.

$$C_D = \frac{F_{Drag}}{\frac{\rho U^2 A}{2}} \tag{6}$$

$$C_L = \frac{F_{Lift}}{\frac{\rho U^2 A}{2}} \tag{7}$$

One of the easiest assumptions that can be made for physical modeling can be to assume the shape of the body or fin to be similar to an airfoil. This assumption has been made for Fin Oscillation and Fin Undulation categories (Khalid et al., 2016; Blevins and Lauder, 2012; Moored and Bart-Smith; Prats, 2015). However, this assumption is most commonly made for Fin Oscillation (Bergmann and Lollo, 2011). Thrust production has been studied not only for an oscillating airfoil but also for a finite shape with flexibility over the span or chord length (Bergmann and Lollo, 2011; Khalid et al., 2016). An airfoil inspired robot using a rigid body oscillation to generate thrust is considered by Pollard et al. (Pollard and Tallapragada, 2017).

4. Hydrodynamic analyses

The hydrodynamic analyses can be done using numerical or experimental methods. These methods are used to better understand either the two-dimensional or rather the three-dimensional flows (Schosser et al., 2016). Numerical methods are considered for fins or body to determine flow characteristics (Ramamurti et al., 2002; Cui et al., 2017; Bottom et al., 2016; Prats, 2015; Tytell, 2004; Li et al., 2016; Liu et al., 2012; Liu et al., 2015; Hirata et al., 2015; Kodati et al., 2008; Studebaker et al., 2016; Borazjani and Sotiropoulos, 2008; Fish et al., 2016; Borazjani and Sotiropoulos, 2009). The most simplified numerical method that investigated undulatory swimming motion is the waving plate theory (Wu, 1961; Techet et al., 2004). Analyses are performed using the governing equations for fluid flow which are given by (Abbott and Doenhoff, 1959):

$$\nabla \cdot V = 0 \tag{8}$$

$$\frac{\partial \rho}{\partial t} + \frac{\partial(\rho u)}{\partial x} + \frac{\partial(\rho v)}{\partial y} + \frac{\partial(\rho w)}{\partial z} = 0 \tag{9}$$

$$\rho\left(\frac{\partial u}{\partial t} + u\frac{\partial u}{\partial x} + v\frac{\partial u}{\partial y} + w\frac{\partial u}{\partial z}\right) = -\frac{\partial p}{\partial x} + \rho g_x + \mu\left(\frac{\partial^2 u}{\partial x^2} + \frac{\partial^2 u}{\partial y^2} + \frac{\partial^2 u}{\partial z^2}\right) \tag{10}$$

where Eq. (9) is the boundary condition for an incompressible flow, Eq. (10) is the general continuity equation for the fluid, and Eq. (10) is the general Navier-Stokes equation in Cartesian coordinates accounting for the flow in the x-direction. Equation (10) also has two other equations that account for the y- and z-directions. Numerical methods can be performed using a multitude of capable software, including but not limited to OpenFOAM (Ltd, 2011–2018) and ANSYS CFX (Ansys, 2018).

Experimental analysis of fluid flow has been conducted in a still water and flow channel using high speed cameras capable of capturing fluid dynamics (Fermigier, 2017; Lauder, 2011; Behbahani and Tan, 2017). Particle-image velocimetry (PIV), a form of pulse light velocimetry, experiments have been conducted to study the effects that shapes have on a fluid by studying the velocity of particles in the fluid regime being displaced by the shape, as shown in Fig. 12 (Ren et al., 2015; Lauder et al., 2007; Wen and Lauder, 2013; Westerweel, 1997; Adrian, 1991; Lauder et al., 2005). This imaging method is performed using $10^{(9.5-11.5)}$ particles in every cubic meter (Krothapalli, 1991). Another imaging strategy based on smaller marker size is molecular markers like fluorescent ink which can be tracked for individual streamlines and vortices created (Adrian, 1991; Yamamoto, 2017). A molecular marker experiment was considered for the Jellyfish to gather the definite movement of its bell and the vortices the constriction creates (Dabiri et al., 2005). Through identification of particle velocity using PIV, fluid flow characteristics can be determined for the structure of interest. Fig. 12 shows different fluid flow for a BCF fish swimming and one lateral pectoral fin for one instant of that motion. PIV yields areas of higher and lower pressure over the body, the vortices produced, and are helpful in determining the force generated by the body (Babu et al., 2016).

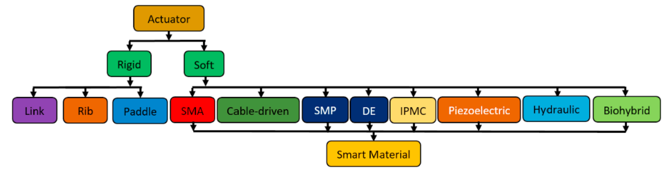

Fig. 13. Actuator flowchart outlining all expressed actuator types.

5. Actuators

By defining the actuators in categories based on their construction, clear motion characteristics can be displayed. Groupings of rigid, soft, and biological components give examples for all the actuators considered, as shown in Fig. 13. In the rigid actuator category, the conventional actuators are described as linked systems that try to replicate the motion of spinal or fin rib structures. The soft actuator category covers soft robotic actuators that could be considered in found systems. Biological actuators are expressed in brief detail as this is the newest category and is still highly experimental.

5.1. Rigid link actuators

The linked systems are considered when the overall components do not deform in size and shape. Actuation is achieved through linkages of rigid component assemblies using electrical motors (Raj and Thakur, 2016). The conception of rigid component actuators capable of performing found motions from the biological or hydrodynamic analyses result in a great variety of designs. These rigid actuators are categorized as follows: single link, multiple link, and fin actuators. Table 1 at the end of this section gives examples for each rigid actuator section.

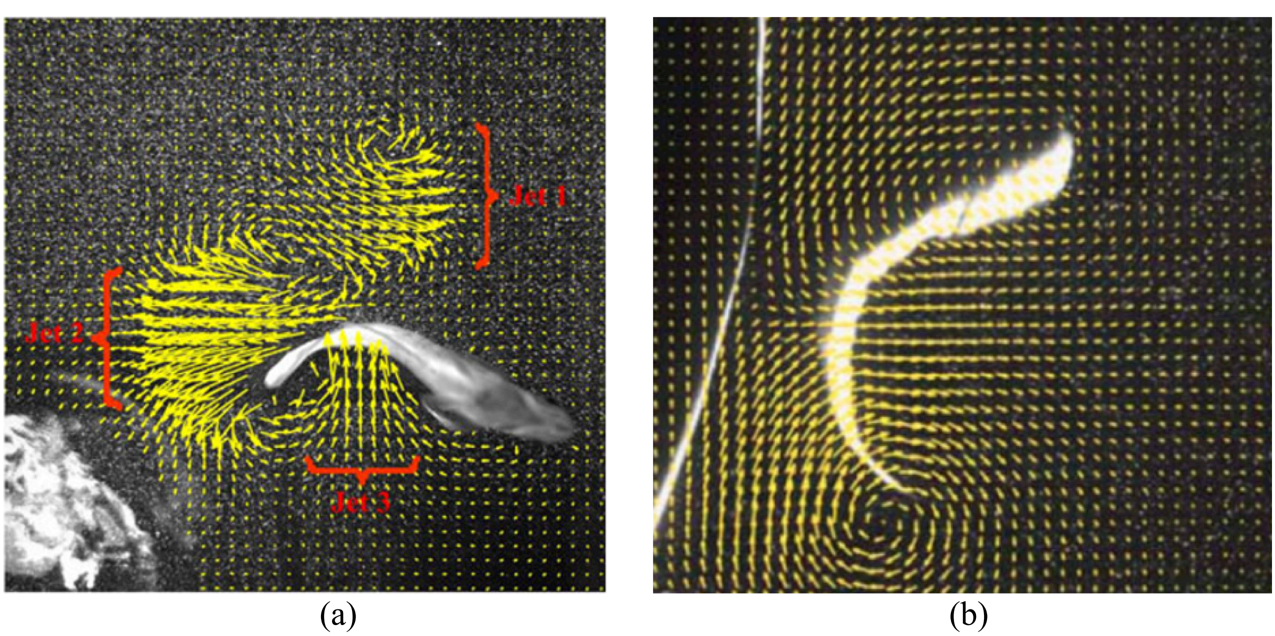

Fig. 12. Velocity fields generated from the PIV marker tracking for (a) a Carangiform fish performing on cycle of oscillation (Lauder, 2011) and (b) pectoral fin motion with a resulting shed vortex off the fin edge (Lauder et al., 2005).

Table 1
Rigid actuator characteristics and pictures of an example system.

Rigid Actuator Type	Characteristics	Pictures
Single Link	• A single motor gives motion to the peduncle unit. • Peduncle section is usually rigid.	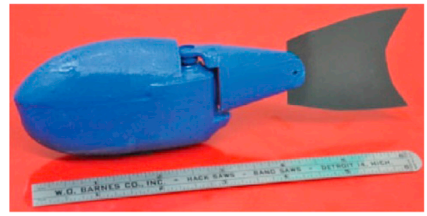 (Kopman and Porfiri, 2013)
Multiple Link	• Multi-link system gives the body more flexibility. • The rigid components are an effective power train.	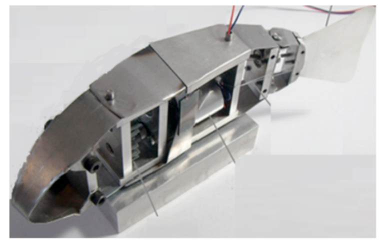 (Clapham and Hu, 2014)
Rib actuator	• **Connected rib actuators** allow for one power source. • Ribs do not have individuality. • Wave motion is congruent over fin.	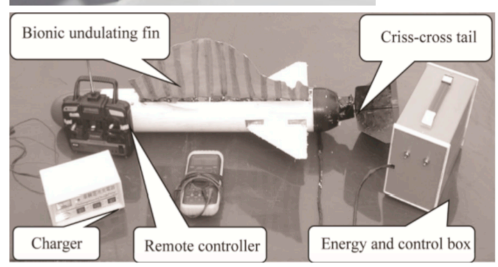 (Xie et al., 2016)
	• **Individual rib actuators** allow for variation of amplitude. • Power is supplied individually so more force can be applied to individual fin sections. • Wave amplitude can be varied for each section.	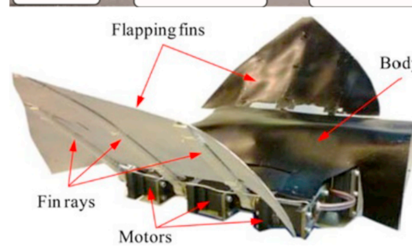 (Zhou and Low, 2012)
	• **The passive fin actuators** are more simplistic compared to individual rib actuators. • These systems have validated systems showing capable thrust and mobility.	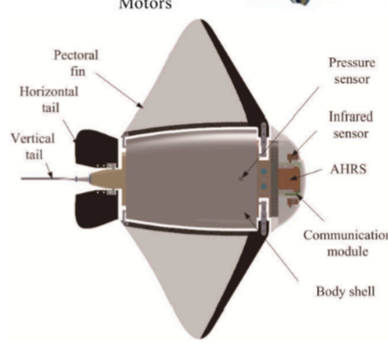 (Niu et al., 2012)

(*continued on next page*)

Table 1 (*continued*)

Rigid Actuator Type	Characteristics	Pictures
Paddle Fin	● The propulsive fins try to replicate the flapping and rowing motion of the Labriform. ● Rowing motion gives more thrust, while the flapping gives more control.	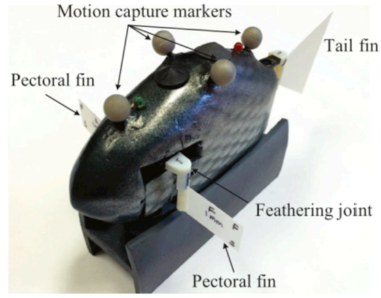 (Behbahani and Tan, 2016)
	● Control paddle fins give caudal fin systems more direction and stability capabilities. ● Multiple motors are needed to create alternative DOF.	 (Shen et al., 2011)

5.1.1. Single link actuator

The single link systems are categorized for the caudal peduncle movement, shown in Fig. 14. This actuator can either have the drive motor in the body or tail section. These actuators are favorable because the thrust is generated from a simple assembly. The reason this actuator type is considered for the Thunniform species because the body undulation expressed by these creatures is restricted to the last section of the peduncle (Kopman and Porfiri, 2013; Marras and Porfiri, 2012). This peduncle restriction is also expressed by the Osctraciiform and Labriform AUV tail motion (Wang et al., 2013; Wang et al., 2014; Lachat et al., 2006; Behbahani and Tan, 2016; Wang and Xie, 2014).

5.1.2. Multiple link actuator

The multi-link actuators give the peduncle a smoother curvature compared to the single link, shown in Fig. 15. The more links used in the actuation the smoother the curve is, as each link equivalates to an increase in joints. The joints can be designed to have a single plane of freedom, where the peduncle unit can move in a lateral or vertical motion relative to the bodies neutral position, respectively (Clapham and Hu, 2014; Liu et al., 2005; Tolkoff, 1999; Suebsaiprom et al., 2016; Hu et al., 2006; Liu and Hu, 2010; Yu et al., 2004; Koca et al., 2016; Yu et al., 2012; Ichikizaki and Yamamoto, 2007; Liu and Hu, 2005; Su et al., 2014; Wen et al., 2012; Yu et al., 2016b; Liljeback et al., 2014; Shen et al., 2011; Anderson and Chhabra, 2002; Stefanini et al., 2012). The Anguilliform category has the highest number of links, usually more than six, while the Carangiform category regularly has five. However, one of the pioneer experimental designs, the RoboTuna used more than five links powered by pulleys to achieve oscillation (Tolkoff, 1999). Power inputs for the multi-link actuators are either the direct current (DC) motors or servomotors housed on each of these joints or at the base of the peduncle (Chu and Zhu, 2016). A unique multi-link Anguilliform robot was created using magnets to attract and repulse each link (Manfredi et al., 2013). Multi-link actuators allow the inclusion of joints that can give the tail another degree of freedom for more flexibility. A more flexible peduncle gives the tail more directional thrust capabilities, and therefore more maneuvering capabilities (Ichikizaki and Yamamoto, 2007; Yu and Wei, 2013; Yu et al., 2009; Rollinson et al., 2014).

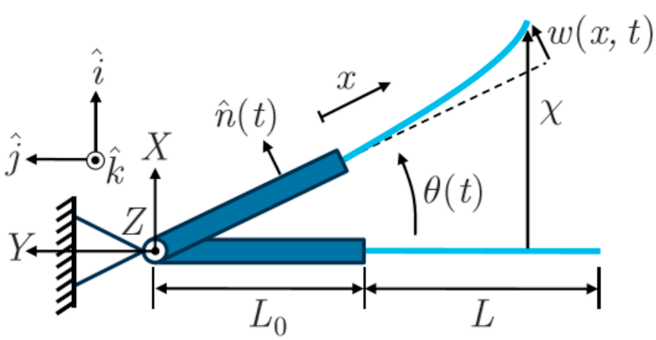

Fig. 14. Simulated single link matching the model for the motion using flexible fin and the resulting Thunniform robot (Kopman and Porfiri, 2013).

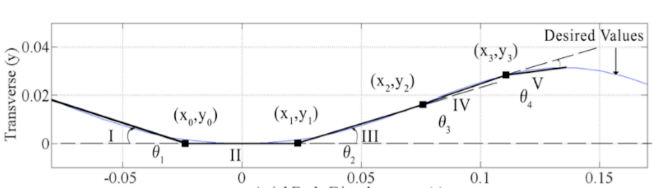

Fig. 15. Simulated link matching to the model for the body and fin motion.

5.1.3. Fin actuators

The fin actuators are considered for the systems that mimic Rajiform, Labriform, and Ostraciiform species. These systems vary between rib actuators and rigid paddle fin actuators. The rib actuators give the wave propagation along the fin while the paddle fin considers the surface to be rigid. The flexibility of ribs is dependent on the material, but this actuator is included in this class because designs follow similar methodology as link systems. Paddle fin actuators have been used for control during swimming.

5.1.3.1. Rib actuators. Rib actuators are considered for systems that use individual rays to excite a flexible membrane, as shown in Fig. 16. The rib actuators can be considered in three categories; connected, individual, and passive. The connected ribbed actuators are considered for systems by (Xie et al., 2016; Siahmansouri et al., 2011;

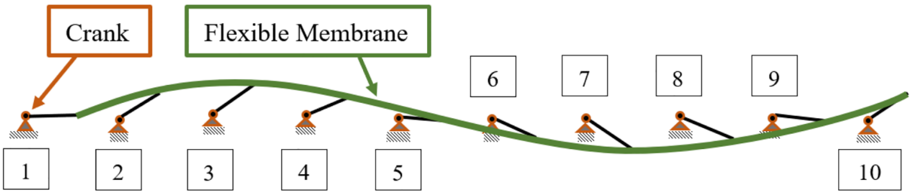

Fig. 16. Example of a multi-rib actuator to cause rib excitation (Low and Willy, 2005).

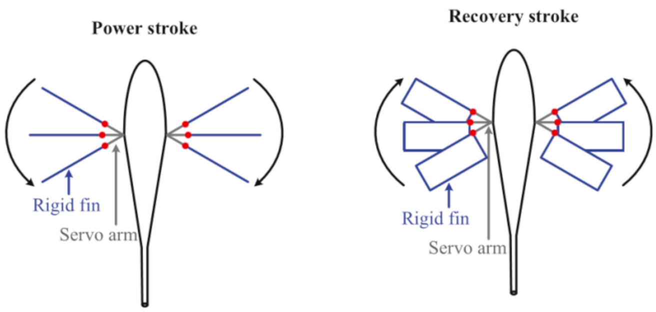

Fig. 17. Paddle fin expressing a complete cycle for a Labriform rowing motion for an AUV with a flexible fin joint (Behbahani and Tan, 2016).

Table 2
Grouping of motors and servomotors found. V is voltage, W is watts, and DC is direct current.

Motor Type	Examples
Servomotor	Hitec 6 V servomotor (Wang et al., 2013)
	60 W class servomotor (Ichikizaki and Yamamoto, 2007)
	HSR-5990TG (Liljeback et al., 2014)
	Futaba 3003 servomotor (Yang et al., 2009)
	17W DC servomotor (Gao et al., 2007)
	HITEC HS-646WP servo (Chew et al., 2015)
	Savox SW1210SG (Gilva et al., 2015)
	HXT900 (Furqan et al., 2017)
	BORCHE's CDS5516 servo motor (Wang et al., 2017b)
DC	16 mm DC motor (Kodati et al., 2008)
	2.83 W Faulhaber DC motor (Lachat et al., 2006)
	RS-550VC DC 12 V/CCW (Liu et al., 2017)
	Solarbotics GM12a DC Motors (Arienti et al., 2015)
	441435 Maxon DC Motor (Arienti et al., 2015)
	RE-max 24 (Yu and Wei, 2013)
	RE10 Maxon motor (Curet et al., 2011)
	Maxon EC-4pole (Wu et al., 2015)
	Escap model 35 NT2 R82 (Mason and Burdick, 2000)

Liu et al., 2017). Individual ribs are considered by (Hu et al., 2009; Yang et al., 2009; Zhou and Low, 2012; Low et al., 2011; Shang et al., 2012; Curet et al., 2011). These ribs are actuated through separate servomotors thus these systems have more than two actuators, as presented Fig. 16. Passive fins are considered by (Liu et al., 2012; Gao et al., 2007; Niu et al., 2012; y Alvarado et al., 2013; Chew et al., 2015; Sfakiotakis and Fasoulas, 2014; Gilva et al., 2015). These AUVs have one or two rigid rib actuators that give undulation to a passive fin membrane. Flexible fin rays were found to increase the efficiency of undulating fin propulsion as it replicated the biological animal (Liu et al., 2017).

5.1.3.2. Paddle fin actuators. The paddle fin actuators are considered for the pectoral fin propulsion and the control surfaces of BCF AUVs. The pectoral fin propulsive actuators are considered for the AUVs created by (Sitorus et al., 2009; Wang et al., 2013; Wang et al., 2014; Kodati et al., 2008; Lachat et al., 2006; Behbahani and Tan, 2016; Zhang et al., 2016; Mainong et al., 2017; Wang et al., 2017a; Castano et al., 2017). The unique paddle fin created by Zhang et al. (Low and Willy, 2005) not only has propulsive pectoral fins but also has a dual caudal fin propulsion that gives this AUV good stability and speed. The AUV created by Kodati et al. (Kodati et al., 2008) supports propulsive pectoral fins that have two degrees of freedom to perform the rowing swimming method, similar to the work of Behbahani et al. (Behbahani and Tan, 2016), as shown in Fig. 17. Fins with 3-DOF are desired, these give the AUV's more maneuvering capabilities (Shen et al., 2011). The control surface paddle fin actuators are considered because they give the craft pitch and roll capabilities (Wen et al., 2012; Anderson and Chhabra, 2002; Wu et al., 2015). To obtain 3-DOF for each fin, a servomotor for each degree of freedom can be applied in the design (Shen et al., 2011). It was described by Behbahani et al. (Behbahani and Tan, 2017) that a variable stiffness paddle fin exhibits much different performance characteristics than a rigid fin.

5.1.4. Motors and servomotors

Direct current motors are considered for these designs as they allow for strong torque and high rotational speeds. Servomotors are also used because they can be rotary or linear actuators (Furqan et al., 2017). A common method to transform the mechanical input of the DC motors into oscillations is to use a Scotch yoke mechanism, rack and pinion or slider crank (Shen et al., 2011; Yu and Wei, 2013). The Fin Undulation uses gear sets to transform the servomotors into useful motion (Wang et al., 2017b). Typical motors used for actuation are found in Table 2.

5.2. Soft robotic actuators

Soft materials have been exploited in almost all categories of locomotion. From all the known soft robotic actuators (SRAs), there are a few types that are capable of motions needed for swimming. The various forms of the smart material actuators will be identified to determine systems that are capable of deformation from a stimulus like electricity. The characteristics of each actuator is shown to discuss later the optimal SRA candidates for AUVs. At the end of this section, Tables 3 and 4 are outlaid in a manner to express the characteristics and physical capabilities of each SRA.

5.2.1. Shape memory alloys

Shape Memory Alloys (SMAs) are smart material actuators that have rising interest in soft robotics. SMA characteristics include high work density, high chemical corrosion resistance, deform locally in the presence of low voltages, fail from cyclic fatigue, movement is hysteric from the complex thermodynamic problem for phase change (Jani et al., 2014; Xiang et al., 2017; Cianchetti, 2013). SMAs go through a material phase shift to use and recover strain potential of the crystalline lattice (Cianchetti, 2013). There are different alloys used as SMAs including copper alloys and ternary alloys, such as NiTiCu, but the most common is the Nickel-Titanium (NiTi) alloy (Jani et al., 2014; Cianchetti, 2013). The preference of this material is its super elasticity (pseudoplasticity) and shape memory effect. Shape memory effect refers to the recovery of the material's original shape after being deformed (Cianchetti, 2013). SMAs can be fabricated in either a wire, beam, or sheet configuration (Cianchetti, 2013). The SMA actuators are continually being developed to try improving their performance (Xiang et al., 2017).

SMAs have been employed in a variety of soft robotic systems with different kinds of movements based on a SMA wire configuration. Many systems developed have been inspired from worms, caterpillars, and octopus. A support structure is needed for the SMA wires, as shown in

Table 3
Actuators' characteristics including stimuli used, what kind of robotic systems use them, and movement produced by these actuators.

Soft Robotic Actuator	Stimuli used	Robotic system(s)	Movement
SMA	Low Voltages	I-Bot (Umedachi et al., 2016)	● Peristaltic movement
		Meshworm (Seoket. al., 2010)	● Peristaltic movement
		GoQbot (Lin et al., 2011)	● Ballistic rolling locomotion
		Softworm (Boxerbaum et al., 2012)	● Peristaltic movement
		Octopus-arm (Laschi et al., 2012)	● Bending
		OCTOPUS Robot (SMA + Cable-driven) (Cianchetti, 2013)	● Jet Propulsion
			● Legged locomotion
BISMAC	High currents	Robojelly (VIllanueva et al., 2013)	● Bell Constriction
Cable-driven	Motors controlling the cables or pneumatic pressure	PoseiDrone (Arienti et al., 2015)	● Jet Propulsion
			● Legged locomotion
		Rajiform Robot (Cai et al., 2009)	● Fin Undulation
		Robot Shark (Lau et al., 2015)	● Fin Oscillation
		Robotic Fish (Zhong et al., 2017)	● Fin Oscillation
		Feather sea star robot (Francis et al., 2015)	● Jet Propulsion
SMP	Chemical or thermal, light, and magnetic fields	–	–
DE	High voltages	MERbots (Mirfakhrai et al., 2007)	● Walking
		Soft Jellyfish (Godaba et al., 2016)	● Jet Propulsion
Ionic Polymer Metallic Composites	Low voltages	Robot Jellyfish (Trabia et al., 2016)	● Jet Propulsion
Piezoelectric	Low voltages	Untethered Caudal Fin (Cen and Erturk, 2013)	● Fin Oscillation
Hydraulic	Pressurized fluid	Soft Robotic Fish (Marchese et al., 2014)	● Fin Oscillation

Fig. 18. A flexible nylon mesh structure is used, but other elastomers have also been implemented (Cianchetti et al., 2012; Follador et al., 2012). The wires must be inlayed in this support matrix to create directional deformation and force. The selection of direction depends on the flexion and recovery that is trying to be achieved.

Circumferential and longitudinal SMA wires, shown in Fig. 18(a) and (b), are implemented to mimic the muscles of a worm that elongate and shorten the body. Circumferential wires contract to decrease diameter thus lengthening the body. Counteractively, its length is shortened by the longitudinal wires contracting which increases the diameter thus shortening the body. The body does not bend, it only exhibits elongation and contraction which produces a peristaltic movement (Cianchetti et al., 2012; Follador et al., 2012; Seok et al., 2013). An octopus-like robotic arm was also developed using radial and longitudinal SMA springs. The radial SMA springs constricts the radius and increases the arm to its original length. Fig. 18(c) shows the radial system set up using SMA springs. Asymmetric position of wire can cause bending for a respective system.

The I-bot, inspired from a caterpillar, uses two SMA coils on one side of the silicone body when activated independently causing an inchworm motion. This motion is initiated by a bending wave in the posterior part of the system tilting the contact angle of the rear foot. When the threshold angle for friction is exceeded, the rear foot is dragged forwards (Umedachi et al., 2016). Another caterpillar-based robot is the GoQbot. SMA coil actuators within silicone are activated simultaneously to constrict the body into a circle causing a ballistic rolling motion (Trimmer et al., 2013; Lin et al., 2011; Laschi et al., 2016).

Wang et al., 2009 designed a micro mimetic manta ray robotic system actuated with SMA wires running longitudinally in an elastomer beam. This beam is a flexible leading edge fin rib that gives undulations to a passive fin membrane. The SMA causes flexion in the beam because it is inlaid in the polymer off the neutral axis and when it is activated, the shrinkage causes the bending in favor of the activated side (Kim et al., 2016). Kim et al. (Kim et al., 2016) devised a design based on a polymer matrix inlaid with a plastic to encourage a vertical flexion.

A biomimetic cuttlefish robot designed by Wang et al. (Wang et al., 2011) and fabricated by Gao et al. (Gao et al., 2014) uses SMA wires for the undulated fin and the mantel constriction of the system. The undulatory fin serves for slow swimming while the mantle is for higher speed jet propulsion (Wang et al., 2011). The undulating fin works using SMA wires distributed throughout the membrane. The SMA wires in the mantel are circumferential, allowing constriction of the mantel cavity (Gao et al., 2014).

Another SMA category named bio-inspired shape memory alloy composite actuators (BISMAC) actuators was used. It can convert the high force and low-strain of SMA wire to a lower-force with larger bending deformations (Smith et al., 2010). The structure of this actuator is composed of the most common NiTi alloy SMA wire, and a thin medium carbon steel fixed in silicone, as shown in Fig. 19 (Smith et al., 2010). This actuator has the ability of being configured to different deformation profiles. Although BISMAC actuator can reach a larger deformation, it still has hysteresis and delay when changing to its original position (Villanueva et al., 2010). Smith et al. (Smith et al., 2010) were able to analyze the reflective points on the actuator. They recorded a maximum deformation of 93.4%–100% by using 4 SMA wires while there was almost no change by adding 3 to 6 wires (Smith et al., 2010).

Robojelly is a bioinspired jellyfish robot designed and fabricated by Villanueva et al. (VIllanueva et al., 2013), that replicates shape and motion of the Aurelia aurita Jellyfish. The required deformation of 44% for the Aurelia aurita. Using single SMA wires alone, it would not function to replicate the contraction since they can only deform by 4% (VIllanueva et al., 2013). The fabricated Robojelly consists of 8 BISMAC actuators fixed inside the RTV silicone bell (VIllanueva et al., 2013).

Table 4
Characteristics of actuators' flexion with pictures of how they make the robotic systems move.

Actuator	Description	Picture of Movement
Shape Memory Alloy	• Crawling is produced by activating the posterior actuator. • When the threshold angle is exceeded, the rear foot is dragged forwards.	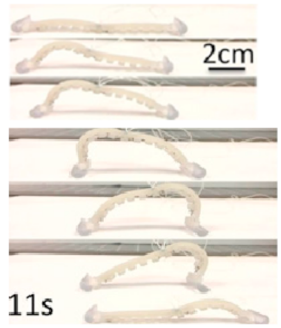 (Umedachi et al., 2016)
	• Peristaltic locomotion is obtained by contracting and lengthing sections of its body using circumfrential and longitudinal wires. • Has the ability to move through small crevices. • In this case, bending occurs by the off neutral axis placement of the wires.	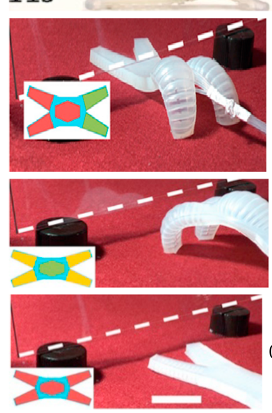 (Laschi et al., 2016)
	• Produces ballistic rolling locomotion due to stored elastic energy. • It has a elongated narrow body mad of silicone actuated by longitudal SMA that can force the body to contract into a circle.	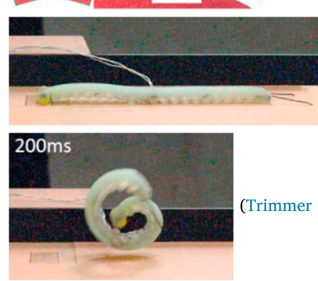 (Trimmer et al., 2013)
	• Uses seven radial SMA actuators inside the mesh arm. • SMA activation elongates the arm and also stiffens it.	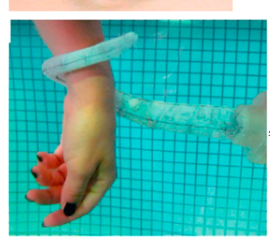, 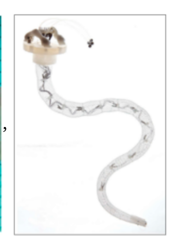 (Laschi and Cianchetti, 2014)
BISMAC	• Contraction and relaxation of the body replicates Jet Propulsion. • A modified SMA, utilizing spring steel in the design. • Robojelly's silicone matrix bell has eight BISMAC actuators radially distributed. • Spring steel converts the SMA into a higher deformation actuator.	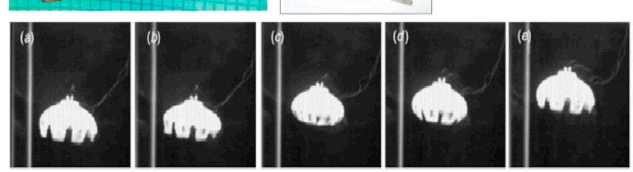 (VIllanueva et al., 2013)
Cable-driven	• Each of its arms has its own actuation mechanism. • Each arm can elongate or stiffen making possible legged locomotion and grabbing objects. • This system incorporates a swimming bladder made using servomotor and wires. • These wires are pulled by the motor contracting the silicone mantle.	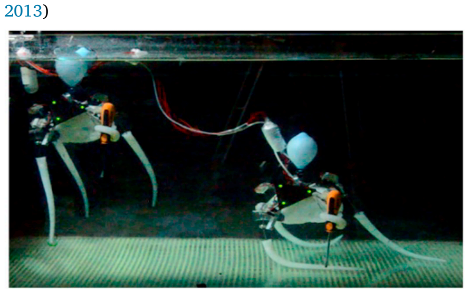 (Arienti et al., 2015)
	• Actuator made of carbon nanotubes.	

(continued on next page)

Table 4 (*continued*)

Actuator	Description	Picture of Movement
Shape Memory Polymer	• Heated when illumination with infrared light.	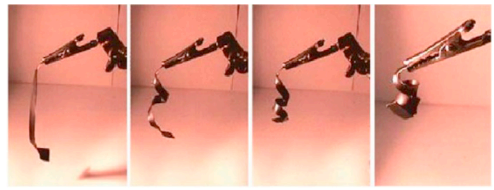 (Behl and Lendlein, 2007)
Dielectric Elastomer	• When the actuator is subjected to voltage the inner bladder expands with air and ejects water from the rigid bell. This expansion increases the buoyancy. • When water is ejected it creates a propulsive force.	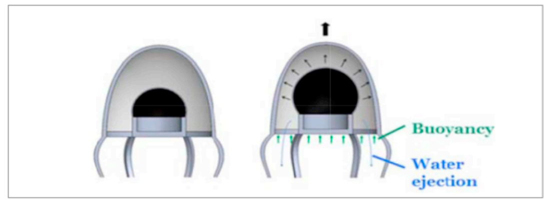 (Godaba et al., 2016)
Ionic Polymer Metallic Composite	• A deformation occurs as a function of time in the presence of a voltage of < 7 V. • When voltage is reduced or cut, the material goes back to its original shape, as the material cools.	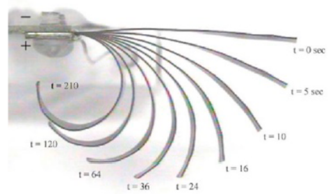 (Mirfakhrai et al., 2007)
Piezoelectric	• Low voltage input. • Low to moderate frequency oscillatory vibration. • High efficiency with moderate power.	 (Cen and Erturk, 2013)
Hydraulic	• Fluidic elastomer actuators (FEAs) produces replicable Fin Oscillation. • Uses anterior trunk actuators to produce a fast forward swimming.	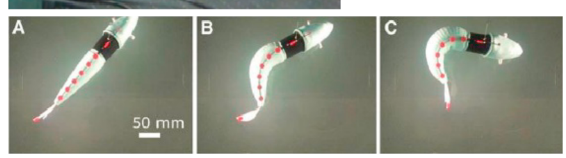 (Marchese et al., 2014)

5.2.2. Cable-driven

Unlike other soft material AUVs presented in this review paper, cable-driven AUVs are powered by servomotors or gas (Marchese et al., 2015; Cai et al., 2009). The function of the servomotors is to produce bending by shortening the wires which causes flexion of the skeletal structure. Wires on each robot have different set up depending on the kind of deformation desired. Fig. 20 shows the longitudinal set up for a robotic fish (Lau et al., 2015), Cownose Ray AUV (Cai et al., 2009), and the radial set up for an octopus inspired Jet Propulsion system (Giorgio-Serchi et al., 2013).

Several robotic systems have been developed using cable-driven actuation. Octopus, Sea Star, and caudal fin species have motions that can be replicated using this actuation. Robot Shark is composed of an elastic beam with six rigid disc links mimicking the fish skeleton with wires running longitudinally down the peduncle, as shown in Fig. 20(a) (Lau et al., 2015). The servomotor on the Robot Shark drives a drum wheel controlling the pull on the wires that cause a bending of the peduncle and oscillates by altering the rotation of the actuator. A robotic fish was created in the same manner but with five discs and complaint last section of the tail with high similarity of motion to the biological (Zhong et al., 2017).

A gas power pneumatic muscle of the flexible foil Cownose Ray AUV contracts a flexible multi-section leading-edge fin rib using rope running on the top side of the rib, as presented in Fig. 20(b). However, this design only capable of a fin upstroke (Cai et al., 2009). By using silicone rubber, the fin span can be given the shape of the fin and giving a high morphology similarity to the biological system (Cai et al., 2009).

PoseiDRONE, inspired from an octopus, combines crawling and jet propulsion mechanisms. The crawling system is made of radially distributed arms each with longitudinal wires running from the motor to the tip of the arm (Giorgio-Serchi et al., 2017). Cables allow each arm to elongate, shorten, and stiffen, which also allows the robot to grab objects. The swimming unit consists of a silicone bladder with a nozzle and ingestion valve (Giorgio-Serchi et al., 2013). This bladder is connected to radially distributed wires, as shown in Fig. 20(c). Once it is filled with fluid, a servomotor pulls these cables contracting the bladder thus producing ejection of the fluid causing thrust. While the bladder returns to its original shape, fluid is being ingested and the ejection process is repeated (Arienti et al., 2015; Giorgio-Serchi et al., 2013). A feather sea star was the inspiration for a soft robot that is composed mostly of linear and circular springs that aid in generating propulsion (Francis et al., 2015; Nir et al., 2012).

5.2.3. Shape memory polymers

Similar to SMAs, Shape Memory Polymers (SMPs) can deform and return to their original shape in the presence of a stimuli. SMPs are an elastic polymer matrix with stimuli-sensitive switches. Although not many AUVs have been made using these kind of actuators, they present characteristics that give them potential. These actuators use other kinds of stimuli rather than electricity, such as chemical, light, and magnetic fields. The shape recovery time of SMP can be a short time for a large deformation range, but larger deformations risk a longer response time (Behl and Lendlein, 2007).

Shape Memory Polymers have many applications, especially for micro-electromechanical systems and actuators in biomedical devices (Trabia et al., 2015; Ricotti and Fujie, 2017). These applications include

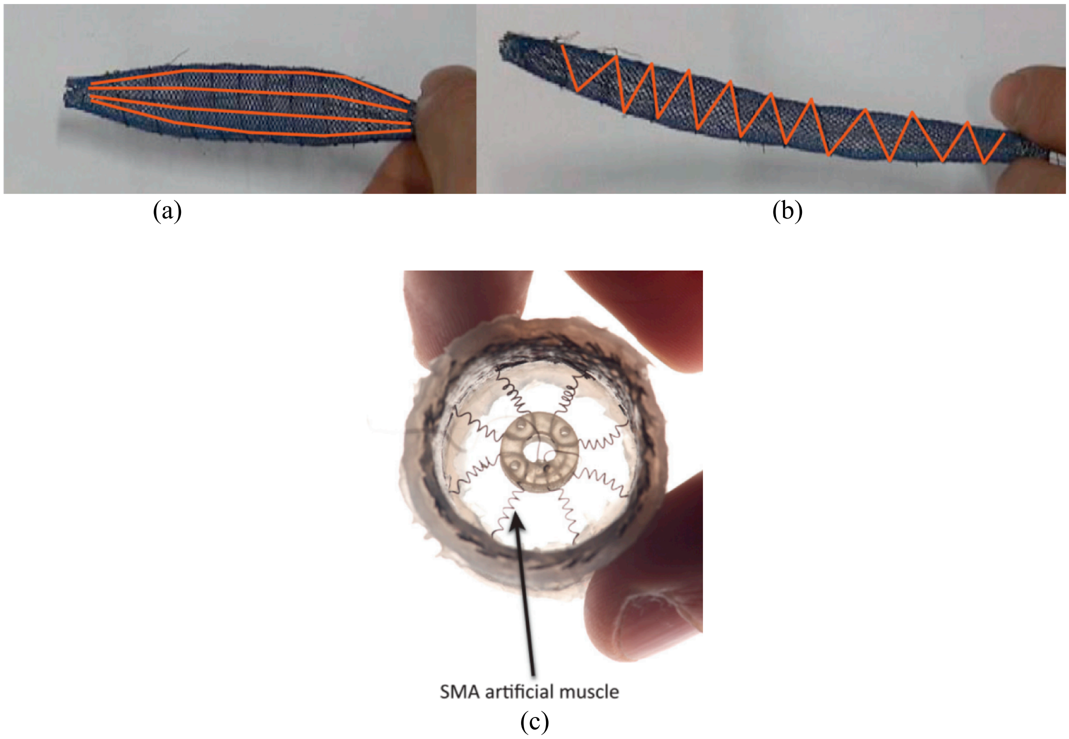

Fig. 18. Mesh structure of a worm-inspired robot showing: (a) longitudinal muscles and (b) circumferential muscles (Trimmer et al., 2013). (c) Inside of the mesh structure used on an octopus-like robot arm showing the radial muscle arrangement (Cianchetti et al., 2012).

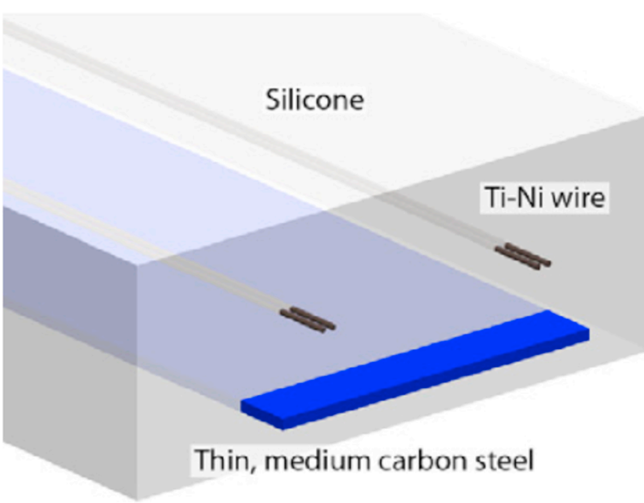

Fig. 19. Schematic of the composition of BISMAC actuator. 4 SMA wires are held at a specific distance from a spring steel strip (Smith et al., 2010).

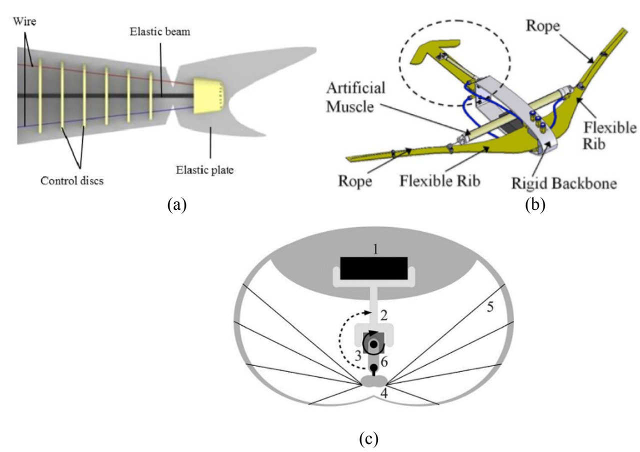

Fig. 20. Cable set up for (a) Robot Shark (Lau et al., 2015), (b) a Rajiform robot with flexible leading-edge rib (Cai et al., 2009), and (c) the silicone swimming bladder used in the PoseiDRONE (Giorgio-Serchi et al., 2013).

laser-activated device that can remove blood clots to biodegradable implants that inflate to help control appetite to reduce obesity (Behl and Lendlein, 2007). These polymers have been considered as better substitutes to metallic materials due to their biocompatibility and flexibility giving them the capability to be used in other applications (Laschi and Cianchetti, 2014).

5.2.4. *Electroactive polymers*

Electroactive Polymer (EAP) actuators are excited through electrical stimulus and they are classified into electronic (dielectric elastomers) and ionic (ionic polymer metallic composites) (Trivedi et al., 2008). EAPs have characteristics, such as low weight, fracture tolerance, and large actuation strain. Dielectric elastomers require high voltage to operate but they have a quicker response and produce large strains.

5.2.4.1. Dielectric elastomers. Dielectric Elastomers (DE) have resemblance to animal muscles based on strain, pressure, density, efficiency, and speed (Pelrine et al., 2002a). When voltage is applied to the electrodes, the opposite charges in the electrodes attract each other generating stress in the dielectrics. This stress causes deformation in the DE in the form of a compression and lateral expansion (Mirfakhrai et al., 2007).

A SRA inspired by a jellyfish was created using dielectric elastomers. This system has an air chamber connected one end to a DE membrane, and the other end is a valve that pumps air in when the DE expands (Godaba et al., 2016). The DE membrane is filled by a defined amount of air. The DE in this case is stimulated when voltage is applied on the actuator, the membrane expands increasing its air volume which helps the system to float. The jellyfish robot generates propulsion by ejecting water and by expanding the DE membrane creating thrust.

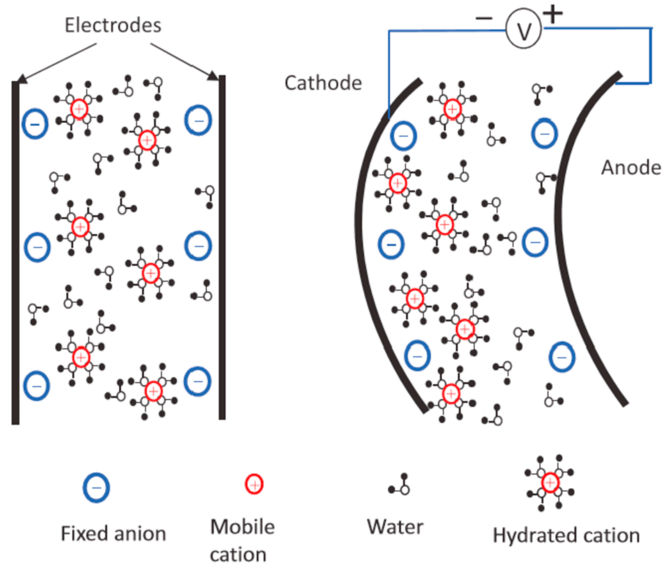

Fig. 21. Ionic polymer metal composite material actuation characteristics (Chen et al., 2012).

5.2.4.2. Ionic polymer metallic composites. Ionic Polymer Metallic Composites (IPMCs) can be used when deformations, such as bending and twisting are needed in design (Trabia et al., 2016). IPMC using voltage as stimuli will be explained. Besides electricity, these materials can also be stimulated by chemicals, light, and magnetic fields (Chen et al., 2012). They consist of a polyelectrolyte membrane in between metallic electrode (Chen et al., 2012). This membrane contains a proportionate number of anions and cations in the membrane matrix. When voltage is applied, cations move to the negatively charged electrode causing an imbalance in the structure. Fig. 21 shows a high concentration of cations on just one side causes the deformation in the actuator but it does not produce a strong force (Pelrine et al., 2002a; Chen et al., 2012).

The bioinspired jellyfish robot designed and fabricated by Najem et al. (Najem et al., 2012) uses IPMC actuators to mimic the propulsion of the Aequorea victoria Jellyfish due to its similarities with the motion of the bell. To achieve the curved shape of the bell, DC voltage was applied to the four IPMC (Najem et al., 2012). A second system utilizing IPMC actuators to mimic locomotion of biological jellyfish is the biomimetic jellyfish robot designed by Yeom and Oh (Yeom and Oh, 2009). Unlike the first robotic system, the IPMC actuators for this robotic jellyfish have been given a thermal treatment of 80 °C for 1 h which allowed for a better flexion (Yeom and Oh, 2009). Yeom and Oh (Yeom and Oh, 2009) stated that applying DC voltage to a flat IPMC actuator could not hold for a constant curvature and its return to original shape is hysteric. In this design, an input signal was implemented in the robot to mimic the rapid changes between the fast-pulse phase and the slow-recovery phase (Yeom and Oh, 2009).

Chen et al. (Chen et al., 2010) introduced the concept of a biomimetic robotic fish actuated by IPMC actuators. A plastic caudal fin was designed to be attached to the IPMC beam to provide the thrust (Chen et al., 2010). The implementation of a wider beam would cause a curling effect instead of bending deformation, therefore, the beam length is an important factor in the design (Chen et al., 2012).

Robotic Rajiforms also utilize IPMC in place of the rib actuators. Individual strips are integrated into a polymer sheet, and are activated

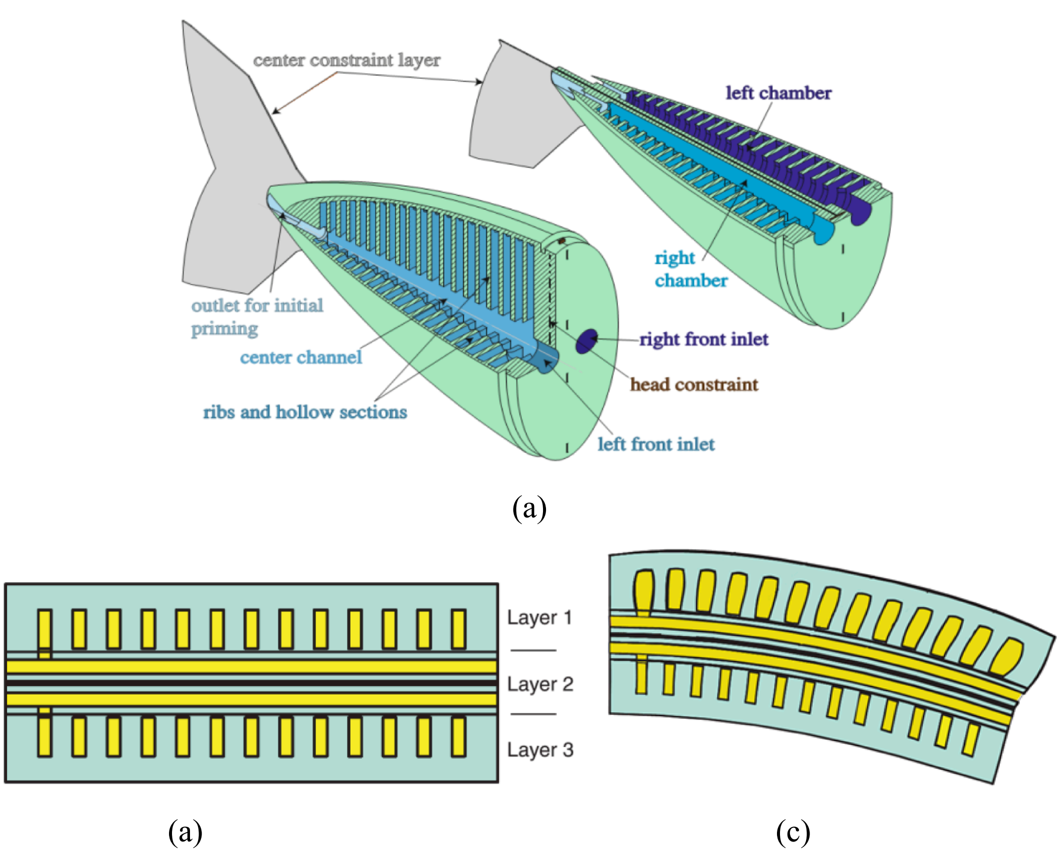

Fig. 22. Representation of a rib segment composed of fluid channels and soft material used in a robotic fish. (a) Two different views of the tail of a robotic fish showing the fluidic actuators (Katzschmann et al., 2016). (b) This segment is composed of three layers. Layers 1 and 3 are the fluidic channels, and layer 2 is the fluid transmission lines (Marchese et al., 2015). (c) Shows the upper fluid channels being filled bending the material (Marchese et al., 2015; Marchese et al., 2014).

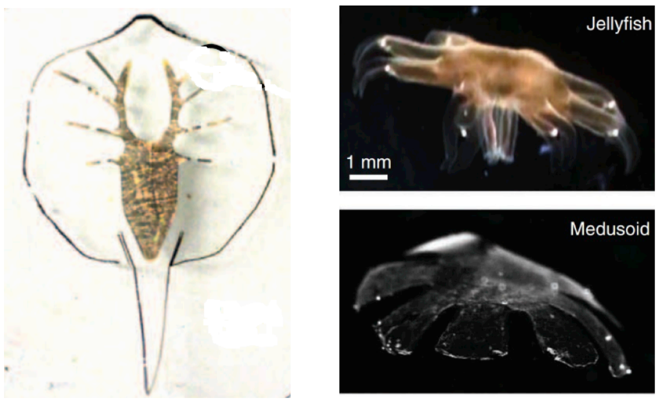

(a) (b)

Fig. 23. Examples of the biohybrid robots (a) robotic stingray (Park et al., 2016) and (b) Medusoid (Nawroth et al., 2012).

to cause the wave propagations from the sequenced bending of the IPMC. Chen et al. (Chen et al., 2012) created a bioinspired robotic Manta Ray using two pectoral fins fabricated by a single IPMC beam actuator with a passive fin membrane (Chen et al., 2012). Punning et al. (Punning et al., 2004) and Takagi et al. (Takagi et al., 2006) created multi-rib IPMC actuators but found that it was difficult to cause the complex wave undulations through selective activation.

5.2.5. Piezoelectric materials

Piezoelectric material is a smart material and has applications for AUVs because it vibrates at lower frequencies using low voltage electric excitation. Applicable piezoelectric material is a macro-fiber composite (MFC) actuator. MFC materials are composed of CTS Wireless Components 3195HD lead-zirconate-titanate that was bound by epoxy (High and Wilkie, 2003). MFC has low strain properties during vibration but the stress is moderate. They work as cantilever beams and have been implemented into caudal fin designs due to the oscillatory vibration. This type of smart material actuators show promise because they bend in plane directions freely and do not exhibit fatigue failure during long cycles. Moreover, this actuator does generate heat.

Only one AUV has been found to have used the piezoelectric actuator. Work by Cen and Erturk (Cen and Erturk, 2013) created a piezoelectric actuator caudal fin. The piezoelectric material was fixed to a rigid body that housed all the batteries and electrical components.

5.2.6. Hydraulic pressure

Channels in an elastomer matrix are put under stress using hydraulic pressure, shown in Fig. 22(a) (Marchese et al., 2015). Consequently, strain is produced and bending occurs, as shown in Fig. 22(b) and (c). These actuators can be manipulated to generate the desired stress by controlling the amount and which channels the fluid goes through (Marchese et al., 2015; Marchese et al., 2014).

Soft robotic fish where the peduncle is composed entirely of Fluidic Elastomer Actuators (FEAs) have been developed. One design has a hydraulic pump that includes a gas regulation mechanism and a delivery system to control the fluid pressure (Onal et al., 2011). The FEA fish by Marchese et al. (Marchese et al., 2014) can reach a maximum bending angle of 100° using the anterior and posterior agonistic and antagonistic body actuators. Katzschmann et al. (Katzschmann et al., 2016; Katzschmann et al., 2018) developed a very capable system that performed an endurance mission in a real-world mission in an oceanic environment.

The Vorticity Control Unmanned Undersea Vehicle (VCUUV) is a solid multi-link actuated robot, and was inspired by the RoboTuna made by Massachusetts Institute and Technology researchers. The VCUUV's hydraulic actuator has multiple tubes connected to each link in the chain to create a powerful motion. This robot is a unique design where no other system found was this large or used rigid links actuated by hydraulic pressure (Anderson and Chhabra, 2002).

5.3. Biohybrid actuators

The biohybrid actuator refers to an integration of muscular tissue and artificial structures capable of imitating the performance of living structures with regards to stiffness and contraction phases (Ricotti and Fujie, 2017; Park et al., 2016; Ricotti and Menciassi, 2012). This type of actuator would allow for greater adaptation, flexibility, and power to soft robots (Ricotti and Fujie, 2017). In addition, they can operate at high efficiency and harvest energy from the nutrients available from their surroundings (Park et al., 2016). Biohybrid actuators can show a higher efficiency over the standard artificial actuators because muscle has a high power to weight ratio (Ricotti and Fujie, 2017). These actuators are constructed by applying a nano-scale thickness of membrane improves muscle contractions for these actuators because muscle bundles must be small layers to this point (Ricotti and Fujie, 2017).

Park et al. (Park et al., 2016) designed and fabricated a robotic stingray utilizing photonic excited biohybrid actuator which had reproducible fin undulation motion capable turning scenarios, as depicted in Fig. 23(a). This system creates coordinated undulating fin motion and phototactically controlled motion using a sensory-motor system (Park et al., 2016). The composition of the biohybrid system includes a 3D elastomer body, a gold-skeleton, an interstitial elastomer coating, and a layer of cardiomyocytes in a body that was smaller than a penny (Park et al., 2016). The thin gold skeleton stores elastic energy during the stroke and rebounds during the relaxation phase, which reduced the complexity of the design (Park et al., 2016).

Nawroth et al. (Nawroth et al., 2012) worked on the fabrication of a tissue-engineered jellyfish inspired by the Aurelia aurita, as presented in Fig. 23(b). The motion of the system was derived by applying electrical impulses to the bell, thus, giving a synchronized movement (Nawroth et al., 2012). The composition of the Medusoid is based on a combination of anisotropic cardiomyocytes and an elastic silicone (Nawroth et al., 2012). The sheet of muscle tissue contracted the bell, and an elastomer returns to original shape (Nawroth et al., 2012). Due to the lack of controlling the muscle contraction, the robotic jellyfish could not achieve the turning and maneuvering tasks (Nawroth et al., 2012).

6. Materials

Material selection is broad and is dependent on the type of actuator selected. As stated, these materials are separated into two categories, rigid and soft. These groups organized the important material properties: elasticity/stiffness, yield, ultimate tensile strength, ductility, hardness, toughness, fatigue strength/endurance limit, and creep resistance. These properties must be considered when designing systems based on their actuator.

6.1. Rigid materials

Found rigid components are grouped together based on their higher stiffness. These materials do not exhibit high elastic deformation. Selection is based off cost of design, motion of actuation, machining capabilities to produce the desired shape, and specified biological characteristics to replicate. To machine complex parts computer-aided manufacturing (CAM) machine tools are utilized because low tolerance of materials is needed. Generally, rigid materials are used for larger components that can handle a higher amount of stress and the desired elastic deformation to be extremely low. These materials are grouped in Table 5. Some of these rigid materials can exhibit flexibility depending on structure where they will be used like fin ribs that are desired to have some complacence.

Table 5
List of found rigid materials. * Specifies a material that might not have high stiffness, and is considered in both rigid and soft material.

Rigid Material	Type and References
Metals	• Aluminum (Clapham and Hu, 2014; Yu et al., 2004; Gao et al., 2007; Gilva et al., 2015)
	• Mild Steel (Clapham and Hu, 2014)
	• Stainless Steel (Clapham and Hu, 2014; Liu et al., 2017; Curet et al., 2011)
Plastic	• *Polypropylene (Clapham and Hu, 2014; Zhou and Low, 2012)
	• Polystyrene (Clapham and Hu, 2014; Ichikizaki and Yamamoto, 2007)
	• Polyvinyl chloride (PVC) (Wang et al., 2009; Gilva et al., 2015; Yu et al., 2014)
	• *Polyurethane (Liu et al., 2017; Yu et al., 2014; Bonnet et al., 2017)
	• *Polytetraflouroethylene (Teflon) (Low et al., 2011)
	• Polymehyl methacrylate (plexiglass) (Gilva et al., 2015)
	• Delrin actural resin (Liu et al., 2017)
	• *Polyethylene (Liu et al., 2017)
Composite	• Carbon Fiber (Gao et al., 2007; Niu et al., 2012)

Table 6
Comparison of soft material actuators relative to strain, stress, and efficiency.

Soft Material	Strain (%)	Stress (MPa)	Efficiency (%)
SMA (Bhandari et al., 2012)	> 4	> 300	> 3.8
Dielectric Elastomer	10-100 (Godaba et al., 2016)	.012-.3 (Pelrine et al., 2002b)	–
IPMC (Bhandari et al., 2012)	> 40	.3	> 30
Piezoelectric (Bhandari et al., 2012)	0.1	35	> 75

Table 7
Used soft materials for AUVs fabrication.

Elastic Material	Type and References
Rubber	• Silicone (Cianchetti, 2013; Trimmer et al., 2013; VIllanueva et al., 2013; Giorgio-Serchi et al., 2013; Giorgio-Serchi et al., 2017; Marchese et al., 2014; Trabia et al., 2016)
	• Rubber Material (Umedachi et al., 2016)
	• Latex (Lau et al., 2015)
Metals	• Spring steel (Villanueva et al., 2010)
	• Cables (Lau et al., 2015; Giorgio-Serchi et al., 2017; Francis et al., 2015)

6.2. Soft materials

Soft materials include materials that can express large elastic deformations and can return to original shape. Deformation can either happen passively or through impulse to the material like electricity. The utility of these materials is that they can bend with the desired motion. Rubber materials like silicone can be used to waterproof and protect actuators. Elastomers can be used to encase moving components like fins and behave similarly to biological animals. The soft material actuators are grouped in Table 6 to show material characteristics. General soft materials are grouped in Table 7.

7. Sensors

Sensors play an important role in giving systems sense of their environment, orientation, and offer utility. Like animals, AUVs need to be able to recognize and adapt to their surroundings, maintain control, and take sample data. Obstacle recognition, position, depth, pressure, stability, acceleration, inertia, force, torque, system electrical current usage, system water leakage, water temperature, and pH sensors are used by bioinspired and non-bioinspired systems. Decreasing the size of these sensors allows for systems to use more than one, giving the systems a broader range of capabilities. Smaller components fit in the limited body cavity space. There is a wide range of components available for selection to make these systems autonomous. The sensors used are found in Table 8.

Obstacle recognition sensors include infrared, camera, sonar, and electrolocation. Infrared and cameras use light waves to capture underwater bodies. Sonar is the sensing of reflected sound pings emitted from the body (Kanhere, 2017). Electrolocation is the recognition of obstacles due to their alteration of the electronic field (Kanhere, 2017). The most commonly used obstacle detection sensor is the infrared sensor. The lateral line is a sensitive array of sensory organs along the side body of biological animals is used for obstacle awareness from fluid movement (Kanhere, 2017). Lateral line sensor designed by Kottapalli et al. (Kottapalli and Asadnia, 2017) describes a variety of hair cell sensors that can detect fluid flow with high sensitivity. A pressure sensor array was considered by Nelson et al. (Nelson and Mohseni, 2017) and Wang et al. (Wang et al., 2017a) to try to mimic the lateral line, but have yet to implement this array in a bioinspired AUV.

GPS keeps the system swimming between objectives. Stability, acceleration, inertia, force, and torque sensors keep the system stable, verify forces exhibited by the structure, and resulting stresses and torques in the structure. Electrical and water leakage sensors monitor the electrical components to make sure battery life is optimized and the system does not short circuit. Pressure and depth sensors are used to keep systems out of failure depths and swimming at the correct depth.

Data collection sensors are not needed for autonomy, but rather for aquatic surveying options. Sensors included in this group are temperature and pH sensors. These give the capability to test the water column and give useful data points difficult to obtain over large volumes.

8. Batteries

The different types of batteries used are mainly: lithium-polymer, lithium-ion, and nickel-metal hydride. These are rechargeable batteries that each has its own respective composition to separate and store

Table 8
Table of sensors. CCD* is a higher image quality in comparison to CMOS. Some non-bioinspired systems are stated to express that there are sensors being adapted for use in larger systems.

Sensing Capability	AUV Sensor	Utility
Obstacle recognition	• Infrared Sensor (Hu et al., 2006; Yu and Wei, 2013; Low et al., 2011; Niu et al., 2012; Wang et al., 2017a; Bonnet et al., 2017; Wu et al., 2017) • Camera (Wang and Xie, 2014; Yu and Wei, 2013; Wang et al., 2017a; Wu et al., 2017) - CCD* (Wang et al., 2013) - CMOS (Yu et al., 2014) - Light Sensor (Lachat et al., 2006) • Sonar - non-bioinspired (Lee et al., 2017; Pyo et al., 2017) • Electrolocation (Wang et al., 2017c) - non-bioinspired (Neveln et al., 2013; Solberg et al., 2008)	• Obstacle recognition sensors give the capability of evasive maneuvering.
Position Depth/Pressure	• GPS (Wu et al., 2017) • Inclinometer (Hu et al., 2006) • Attitude Transducer (Wu et al., 2015) • Pressure Sensor (Hu et al., 2006; Yu and Wei, 2013; Zhou and Low, 2012; Niu et al., 2012; Wang et al., 2017a; Wang et al., 2017b; Wu et al., 2017)	• Gives mission route swimming capabilities. • Depth control is important for mission objective. • Component housing is subject to failure at great depth.
Stability Acceleration/Inertia	• Gyroscope (Hu et al., 2006; Yu and Wei, 2013; Shang et al., 2012) • Accelerometer (Lachat et al., 2006; Hu et al., 2006; Shang et al., 2012) • Inertial Measurement Unit (Wang et al., 2013; Wang and Xie, 2014; Shang et al., 2012; Wang et al., 2017a; Wu et al., 2017)	• Used to maintain stability of the system. • Acceleration and Inertial sensors determine stability and motion of the system.
Force/Torque	• Strain Gauge (Kodati et al., 2008; Chew et al., 2015; Mainong et al., 2017) - (full or half Wheatstone Bridge) (Liljeback et al., 2014) • Stress sensor (Gao et al., 2007) • (Giorgio-Serchi et al., 2017; Godaba et al., 2016)	• Used to maintain the validity of the system so failure does not occur.
Electric Current	• Voltmeter (Hu et al., 2006) • Current Sensor (Hu et al., 2006)	• Determine battery life and current supply to components.
Water Leakage	• (Lachat et al., 2006)	• Used to protect electronics compartment from devastating failure.
Temperature	• (Wu et al., 2017)	• Temperature gradients can be determined for water column.
Chemical	• pH Sensor (Wu et al., 2017; Ravalli et al., 2017)	• Acidity of the water can be determined for environmental data collection.

Table 9
Batteries used in found AUVs.

Battery Type	Examples
Li-polymer	7.4 volt 1000 mAh Li-Polymer (Chew et al., 2015) 7.3 volt Li-Polymer (Chen et al., 2012) 11.1 volt 1500 mAh Li-Polymer (Wang et al., 2009) 22.2 volt Li-Polymer (Wu et al., 2017)
Li-ion	4.2 volt Li-Ion (Lachat et al., 2006) NCR18650B (Wu et al., 2015)
Ni-metal	1.2 volt NiMH (Kodati et al., 2008) 7.2 volt Ni-MH (Wang and Xie, 2014) 7.2 volt 4500 mAh Ni-MH (Zhou and Low, 2012)
Random	7.4 volt (Gilva et al., 2015) Hornet 360 (Takagi et al., 2006)

charge. The Ni-MH batteries are a cheaper option but do not have long life in comparison with the Li-ion and Li-polymer (Buchmann, 2017). Ni-MH do not have harmful metal compounds so pollution potential is null which is not the case for Li-ion or Li-polymer (Buchmann, 2017). Li-polymer can be made into many sizes, extremely thin or large, but are generally lightweight (Buchmann, 2017). Li-ion has potential to be the most powerful, but is the most expensive of the three exhibited as it is still not manufactured in large scale (Buchmann, 2017). The used batteries for AUVs applications are depicted in Table 9.

9. Critical discussion: constraints, limitations, and future recommendations

All the previous sections show critical background necessary prior to discussing trends and offering our observational comments and future recommendations. A conceived design cycle for AUVs is shown in Fig. 24. This figure is the overview for necessary steps needed to create bioinspired or more preferably biomimetic AUVs. The control units that

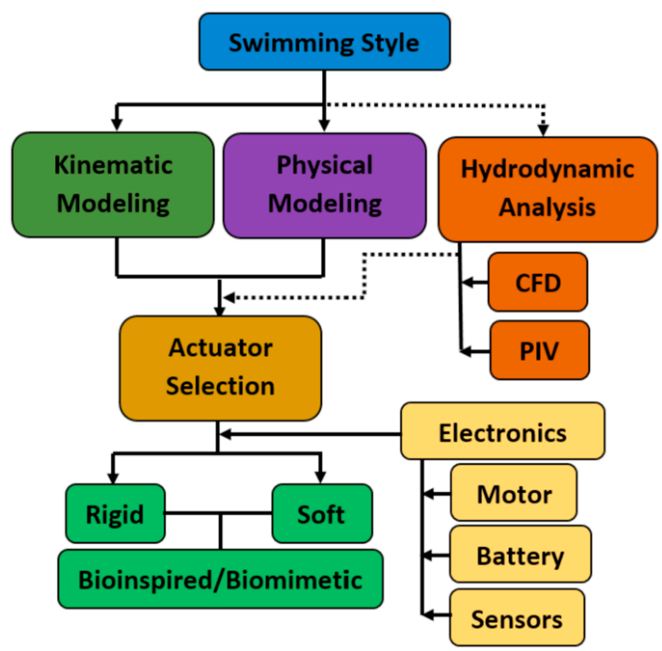

Fig. 24. Schematic of the main topics: kinematic modeling, physical modeling, hydrodynamic analysis, actuator selection, and electronics selection.

should be considered in the electronics selection have not been investigated because they require an in-depth investigation to push the boundaries of autonomy. There are multiple aspects of bioinspiration that lead to more biomimetic designs. Primarily, the selection of the locomotion type and respective animals should have the largest influence in the design. Generally, a design should account for every constraint from the biological animal including sizing, kinematics, physics,

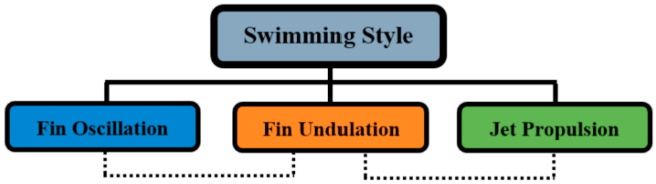

Fig. 25. Types of swimming styles and the combination.

and hydrodynamics. Sizing is not included in this paper as this requires an understanding of multiple case representations for each biological locomotion, as mentioned in (Salazar et al., 2018a). This review gives examples of how the kinematics are derived, obtaining some physical phenomena of the system, and hydrodynamic analyses. All these methods attempt to model the intended system to gain a more fundamental understanding to create a functioning AUV. The actuator selection is dependent on the modeling of the system and the materials desired to replicate the motion and structures of the inspirational animal. The electronics help AUVs be more autonomous and react to their surroundings. Control systems for actuators are not consolidated in this review as they require a separate in depth review. Indeed, control strategies are different for rigid and soft actuators and should be considered post actuator selection. Design recommendations will be made to help lead future investigators to build capable swimming designs.

9.1. Swimming style

First, the desired swimming style must be selected. The main categories are Fin Oscillation, Fin Undulation, and Jet Propulsion, as shown in Fig. 25. Fin Oscillation and Fin Undulation categories utilize similar fins: tail, pectoral, dorsal, and anal. However, Fin Oscillation species that solely utilize the body caudal fin (BCF) exhibit the fastest speeds. Jet Propulsion are characterized for animals that force water out of a constricting volume.

9.2. Kinematic modeling

The kinematics includes determining the body shape and size of the animal and representing the motion of these structures. Caudal fin animals require an understanding of the mechanics of the BCF spinal flexion including head and tail displacement. Pectoral, dorsal, and anal fins necessitate an understanding of the fin edge (leading/trailing) displacement relative to the fin root and how the fin span reacts to the torsion caused by the edge displacement. What has not been implemented into design or study is a combination of pectoral, dorsal, anal, and caudal fins for the Ostraciiform (Li et al., 2016). However, fin kinematics are much more complex than the BCF. In fact, many used models did not include the torsion and large deformation for fin flexibility. Work by Blevins et al. (Blevins and Lauder, 2012) attempts to include these three-dimensional effects of the Rajiform fin. Beam and plate theories can also be modified to attempt to explain these flexible fins.

The animals in Fin Oscillation and Fin Undulation classes have more rigid fin ribs in the membrane. These composite fins increase the fin stiffness and create great propulsive and control surfaces. One thing to note for all these animals is that the body composition and structure determine the rigidity of the body and fins. Bony fish usually have vertebrae and fin ribs, as shown in Table 10. The more vertebrae that the spinal column is segmented into the more flexible and undulatory the body can be. Alternatively, the spine can become more rigid with less joints and transfer powerful concentrated fin strokes. Fin rib rigidity depends on the size and density of the rib. Tail fins tend to have a large number of fins that create semi-rigid structures. If fin ribs have multiple segments, the structure is for sure more flexible. Cartilaginous animals can have individual or interconnected fin rib structures to either give isolated control or structural support. The fin structure of the bony fish are individual fin structures that besides for the caudal fin are attached to the spine. For the Ghost Knife fish, the rib structures of the undulatory fin are segmented and varying in thickness and density. The Gymnotiform's last rib is what these animals use to control the fin membrane. The animals in the Jet Propulsion category lack rigid structures and express large body deformation.

The kinematic modeling needs to adapt to include the flexibility of fins and bodies for these animals. Animals in all the categories exhibit some form of body flexibility. The variation of body flexibility depends on the animal shape, musculature, and skeletal structure. Fins have varying flexibility depending on the composition of excitation structures. Fin Oscillation animals have more rigid fin ribs in the membrane while Fin Undulation animals rib structures are much more flexible. The Jet Propulsion animal's bodies are largely independent of any rigid structures so their bodies are the most flexible out of the three categories.

9.3. Physical modeling

The physical modeling gives the Reynolds number and Strouhal number if frequency of oscillation, length of animal, the amplitude of oscillation, fluid viscosity, and fluid speed are known parameters. However, obtaining the thrust and drag for these systems is more complicated. The pressure and shear stress distribution of the fluid over the body need to be known to obtain these terms. This poses a difficult engineering problem if the exact solution is desired because it requires a complex understanding of the fluid regime. This is done through the hydrodynamic analysis. Assumed generalities about the thrust and drag can be made to obtain the coefficients of thrust and drag. Assumptions about the shape of interest can yield a simplified result for the thrust and drag.

9.4. Hydrodynamic analyses

There are two methods used to understand the fluid mechanics of the system, namely, experimental and numerical. Experimental methods study the biological animals and AUV swimming utilizing PIV. These cameras are capable of tracking velocity of particles. This is extremely useful as it offers a solution for the pressure and shear stress for the fluid regime. The quality of the PIV analysis is dependent on the equipment used, the more expensive units are capable of more detailed sensing. Ultimately, these high speed sensory cameras give flow characteristics to determine the forces on the body which is done by integrating the pressure and wall shear over the shape. This technique also helps to study material response of the AUV during swimming, like similar fin and body morphology to the biological. These methods do not only help to determine constraints of design but also work as a validating step for future work.

The numerical methods are much more tedious in comparison with experimental analysis. These methods use software to complete complex computations where generalities or assumptions are made to obtain a solution. Creating moving structures that are precise replicas of biological structures is difficult in simulations. Analysis using a rigid body are common. For motions like the BCF movement, an assumption of body shape to a symmetric shape airfoil is also common. There are cases of computational fluid dynamics (CFD) analysis for almost all kinds of fish locomotion but, inclusion of body motion with fin motion is rare. The numerical methods are tedious, requiring a good understanding of the structural shape of the animal, the locomotion kinematics, and one must have a firm understanding of fluid dynamics.

9.5. Actuator selection

Creating a perfectly capable AUV is still years away but major advances are being made with actuator development. Actuator selection is

Table 10
Representative skeletal structures for bony/cartilaginous animals.

Category	Comments	Representative picture
Anguilliform	• Body is highly segmented. • Species can have an active or passive dorsal/anal fin. • Efficient undulatory system.	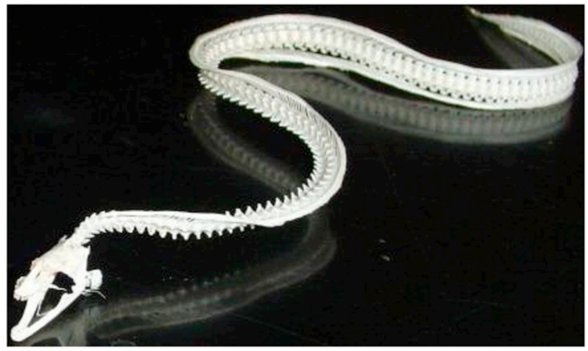 (Moray)
Carangiform	• Less segmented than the Anguilliform. • Fins with individual rib structures are much more pronounced. • Caudal fin is a the largest and is more rigid for thrust.	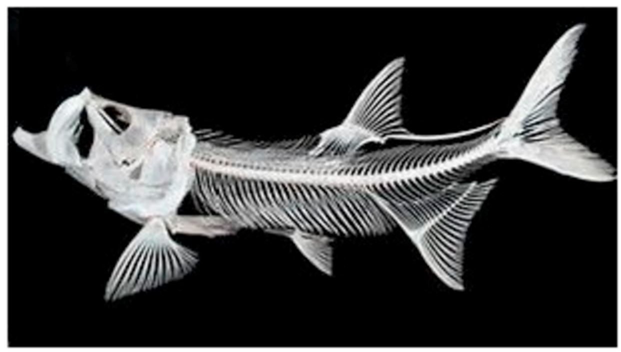 (Tarpon)
Thunniform	• Least segmentation of the spine. • Tail fins exhibit high rigidity on the leading edge of the fin. • Fin ribs are individual structures.	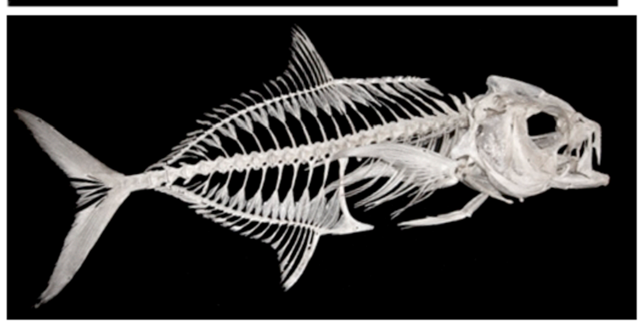 (Pinterest)
Gymnotiform	• Sometimes has body structures similar to the eel. • Fin ribs can be multiple segments which increased willed control of the fin. • Box C indicates the change of thickness between different rib segments of the anal fin.	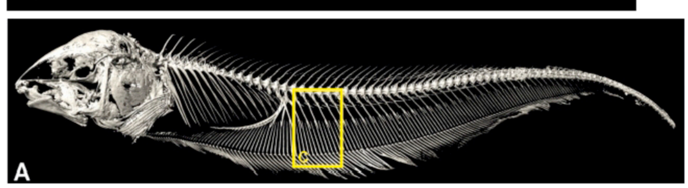 (Youngerman et al., 2014)

(continued on next page)

Table 10 (*continued*)

Category	Comments	Representative picture
Rajiform	• Stringray skeletal structure is very thin cartilage ribs that would support muscular fins. • Increased rib number gives the animal even more control over the fin.	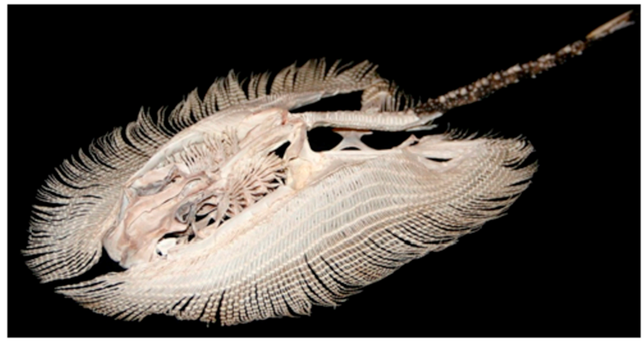 (Salazar et al., 2018a)
	• Cownose Ray cartilage structure is more for support of the fin. • More cross rib support.	 (Salazar et al., 2018a)

difficult because of the complex architecture and motions of the biological animals which actuators need to replicate. This review has described the known actuators that have been or could be included in AUVs to give an expansive representation of the possibilities to be used in design. The actuators have been organized into rigid and soft categories.

9.5.1. Rigid actuators

Rigid actuators have better thrust capabilities as motors provide powerful mechanical input where the body structure is made stronger with rigid links. BCF rigid link actuators try to replicate the spinal flexion but they lack the multi-dimensional spinal flexibility that the animals have. Inclusion of planar joints to the main link chain attempts to replicate this phenomenon but still lacks this flexibility, including another plane of motion to create flexibility. Rigid rib actuators have been shown that they can cause wave propagations in a flexible fin membrane. Tests utilizing more flexible ribs caused higher thrust than the stiffer ribs. Paddle fin actuators have been proven useful in propulsive and maneuvering control. Propulsive paddle fins utilize either flapping or rowing motion, there have not been designs that try and utilize both. Paddle fins used for maneuvering control exhibit the best capabilities when they are capable of more degrees of freedom to control roll and pitch. In Table 11, the advantages and disadvantages of rigid actuators are summarized.

9.5.1.1. Link actuators

Single link is the most simplistic design as there is only one joint that exhibits rotation and requires a single oscillating servomotor. This type of actuator has been used in Thunniform and Ostraciiform designs as these require a more isolated peduncle oscillation to the caudal fin. The issue with these systems is that they lack directional control because the peduncle only has one planar direction of motion. These designs have utilized rigid plastics for the component construction.

The multiple link actuators are much more diverse than the single link. The inclusion of the more joints makes the peduncle more flexible similar to the biological phenomena. This allows the rigid links to match up with the motion model for the backbone of the caudal fin fishes. These links are composed of materials like metals or rigid plastics. The Anguilliform AUVs include many more joints than the Carangiform designs where Carangiforms generally have less than five joints. This limitation for the Carangiform is from the links being restricted to the peduncle section. Anguilliform designs which include more than ten small links like that of Stefanini et al. (Stefanini et al., 2012) creates an extremely flexible body. Carangiform designs like the iSplash incorporate links that are over the whole body that give a more realistic whole-body flexion as it creates a head oscillation (Clapham and Hu, 2014). An issue with including more joints is that the control for the motion becomes more difficult. Studying control methods requires a more exclusive study. The robotic dolphin design by Yu et al. (Yu et al., 2016b) utilized a flexible head joint to mimic head oscillations of a biological dolphin. The inclusion of a head joint in combination with powerful DC motors allowed this design to achieve a fast-enough speed to propel the AUV out of the water. A robotic dolphin by Yu et al. (Yu and Wei, 2013) included a lateral joint at the base of the peduncle giving a different flexion of the peduncle for turning. Researchers are trying to integrate these link systems into traditional propeller based systems to enhance endurance and performance like that in Scaradozzi et al. (Scaradozzi et al., 2017b).

9.5.1.2. Rib actuators

The connected rib actuators utilize a connected crank system, requiring only one mechanical input for this system. The utility of this design is that the control of the wave propagation is based on how the crank design transmits the mechanical energy down the chain. Each rib moves in a perpendicular plane to the body, and oscillates in a singular plane. The issues with this design are that you cannot alter the wave amplitudes along the fin, the motion is fixed to the designed requirements. Only frequency of oscillation can be altered by increasing the

Table 11
Rigid actuators' advantages and disadvantages.

Actuator Type		Input	Advantages	Disadvantages
Linked	Single Link	● One motor	➢ Simple design	➢ Does not have high flexibility ➢ Swimming instability
	Multiple Link	● Powertrain of servomotors	➢ Gives the peduncle a higher degree of flexibility ➢ Similar design to the bony fish skeletons	➢ More links, higher degree of freedom and more flexibility ➢ Coupled chain of links is more difficult to control
Rib (Pectoral, Dorsal/Anal Fin)	Connected Link	● Linked chain with single motor	➢ Crank system performs the same propagation cycle after cycle	➢ Does not have independent fin control like real animals
	Individual Link	● Powertrain of servomotors	➢ Independent fin control ➢ Different amplitudes	➢ More links, higher degree of freedom and more flexibility ➢ Coupled chain of links is more difficult to control ➢ Bodies that hold the electronics and fin rib are rigid, thus the body does not have the flexibility of the biological animals
	Single Rib Passive Fin	● One motor	➢ Less motors but a surface still performs wave propagations ➢ More simple designs with less electronic requirements	➢ Limited control over membrane once undulation wave is created from displacement of leading-edge rib
Paddle Fin (Pectoral Fin)		● Servomotors at the fin base	● Can be used for propulsion or maneuvering control ● More servomotors a higher degree of freedom fin ● Surface can be mostly rigid	● Flexible fins that have a higher degree of freedom are harder to control

input signal for the crank chain. This actuator type does not give the independent rib excitation like the biological animals.

The individual rib actuators have an input motor on each rib that is connected to the body. The servomotors require a control signal to initiate and advance the wave propagation. Like the connected rib actuators, the servomotors cause the rib to rise and plunge in a single plane. The utility of this actuator type is the ability to control the amplitude of each rib, and the direction of the wave propagation. A majority of the AUVs found utilize the individual rib actuators. The difficulty of these systems is that controlling the servomotors in sequential order with the correct amplitude to give the best efficiency requires a deeper understanding of the response of the system. Curet et al. (Curet et al., 2011)created a capable undulatory fin but the body of these designs are rigid. The assemblies of these AUVs lack the spinal rigidity which the inspirational biological animals have.

The single rib passive fins require less motors than the individual rib. The single rib rises and plunges in oscillation like the two other actuators in this class. Then, a travelling wave is transmitted passively across the attached membrane. This actuator type is simple and has already been integrated into a working Rajiform AUV design by Niu et al. (Niu et al., 2012). With future development this actuator could be a good choice as it is simple, requires less motors, but has still proven to be a capable AUV.

9.5.1.3. Paddle fin

The rigid paddle fin actuators have utility for both propulsion and maneuvering control. Propulsive caudal fin designs are usually only planar oscillation similar to the single link design, however, the joint is right at the fin base. These actuators only cause actuation to the fin but because of the aqueous environment the body experiences a torque causing issues with directional control. These single caudal fin actuators tend to cause yaw instability to the AUV. A method to counteract this is to use two caudal paddle fins like the design by Zhang et al. (Zhang et al., 2016). Propulsive pectoral fins are inspired by the Labriform and Ostraciiform rowing and flapping motion. Utilizing planar oscillator paddle fin actuators that have a single degree of freedom for rowing makes them inefficient. Designs, such as Behbahani et al. (Behbahani and Tan, 2016) overcome this high drag by making a flexible feathering joint to replicate the rowing motion of the Labriform.

The paddle fins can also be used as maneuvering control surfaces. Either a one, two or three degree of freedom fin can be created, allowing these AUVs to adjust pitch, roll, and yaw (Shen et al., 2011). Designs that do use the higher degree of freedom do tend to be larger as more actuators or complex mechanism must be integrated around the fin joint. These fins can act as wings and have even been used for gliding to conserve energy during swimming, this can be seen in work done by Wu et al. (Wu et al., 2015).

9.5.2. Soft actuators

Soft robotics can be explained by systems that predominately use elastic materials. For sure there is an amount variation of soft materials used in these AUVs where some components might be solid based. However, the actuators themselves are considered flexible, capable of deformations to achieve locomotion.

Actuators capable of this are SMA, IPMC, piezoelectric, cable-driven, hydraulic, and biohybrid. SMP can bend but have not been implemented into AUV design. DE are capable of expansion but are inefficient for AUVs. SMA are the most powerful smart materials. SMA wires are integrated into a flexible material and is heavily dependent on location of attachment as off neutral axis of attachment causes the bending. Using a spring steel for the BISMAC actuator creates a better bending and return as it can be used for attachment guides. IPMC are more capable at making large deformations but are not as powerful as SMA. Piezoelectric is one of the smart materials that offers a solution for

Table 12
Soft actuators advantages and disadvantages.

Actuator Type	Input	Advantages	Disadvantages
SMA	• Low voltage	➢ High power to weight ratio smart material ➢ Shrinkage is shape memory effect, elongation is deformation	➢ Cyclic fatigue failure ➢ Heat transfer problem ➢ Hysteresis bending and deformation ➢ Low response time
Cable-driven	• Motors controlling the cables • Gas powered pistons	➢ Gives good mimicry for motion ➢ Has been shown to be used in all three locomotion categories ➢ Constant power input from the motors ➢ Capable and more powerful motions	➢ Motion is dependent on assembly design ➢ Fatigue of contact points can happen
SMP	• Chemical or thermal, light, and magnetic fields	➢ Bend deformation	➢ Hysteric bending
DE	• High voltage	➢ Expands to deform ➢ Higher response time	➢ Hysteric deformation
IPMC	• Low voltage	➢ Bending deformation ➢ Fin Oscillation & Undulation	➢ Hysteric bending ➢ Low response time
Piezoelectric	• Low voltage	➢ Oscillatory bending vibration ➢ Efficient with moderate power	➢ Low deformation amplitudes
Hydraulic	• Pressurized fluid from a hydraulic pump	➢ Elastomer based actuators have high deformation ➢ Rigid based actuators can be powerful ➢ Good response time based on actuation set-up	➢ High energy costs for the water pump
Biohybrid	• Musculature stimulus	➢ Have the power efficiency of real muscle ➢ Muscle can be manipulated into designs where a stimulus skeleton can be ingrained next to the muscle	➢ Still highly experimental ➢ Systems are not large ➢ Muscle packaging needs to enlarge

oscillatory bending. Cable-driven actuators depend on the contraction of the wires, and has been shown that it can be implemented into Fin Oscillation, Fin Undulation, and Jet Propulsion designs. The utilization of powerful servomotors with flexible wires and more mimetic body shapes makes these designs a good representation of realizing more mimetic designs. Hydraulic actuators show promise in BCF designs as the completely elastomer peduncle can perform the high flexural oscillatory bending. In Table 12, advantages and disadvantages of soft actuators are consolidated.

9.5.2.1. Shape memory alloys. As it was mentioned before, SMAs raised a lot of interest in the soft robotics field because of their extremely high power to weight ratio and shape memory effect. However, the strain of SMA is low and exhibit fatigue failure on the order of 2×10^7 cycles (Zhang and Sun, 2017). Among the alloys available for these actuators, the NiTi alloys are the best option since they present the best memory and super elasticity. They can be deformed by using low voltages, and have a high resistance to chemical corrosion. These actuators exhibit a control issue that come from the hysteresis of the shape memory effect and cooling. SMAs show less strain and a lower efficiency than the IPMC and piezoelectric.

Different kinds of bending motion can be achieved by SMAs depending on the structure and layout of the SMA. The movement produced by worms is a common type of motion among AUVs fabricated with these actuators. This is because the longitudinal and circumferential/radial SMA wires alternate to cause peristaltic movement. Using circumferential SMA wires makes the robotic system contract its diameter, and longitudinal wires shorten the length of the body. The low strain of the SMA was altered by using a spring steel as a mounting substrate where the SMA has an off axial loading on the spring steel to cause larger bending. This combination is outlined as the BISMAC actuators and was used in Jellyfish AUVs, and can present a good planform for future designs following Villanueva et al. (VIllanueva et al., 2013). It is recommended that this smart material sees improvements in hysteresis control and longer lifespan before reliable long swimming missions can be carried out using this actuator.

9.5.2.2. Cable driven

Unlike other actuators used in soft robotics, cable-driven requires a servomotor or pneumatic pressure to produce the pulling of cables thus causing motion. These inputs are more constant and reliable than a majority of the smart actuators. Like SMA actuators, cables shorten to cause off-axial bending or pull on a membrane. This is the only actuator that has exhibited motion capability in all three classes: Fin Oscillation, Fin Undulation, and Jet Propulsion. The difficulty with these systems is that the motion is a direct correlation of the actuation assembly. The desired motion replication can see great improvements with this class with future development.

A peduncle with flexible links and a compliant caudal fin was created by Zhong et al. (Zhong et al., 2017), and is capable of performing the spatio-temporal function given in Eq. (1) with great similarity. This is one of the best soft designs capable of Fin Oscillation. A flexible leading-edge fin rib with a passive undulating fin was created by Cai et al. (Cai et al., 2009). This design used pneumatic stimulus to pull on a rope that ran over the top of the flexible fin rib. However, this system could perform only an upstroke motion. Investigation should be done to create a downstroke for this design as then it would be more mimetic. A mantel compression bladder was constructed by Giorgio-Serchi et al. (Giorgio-Serchi et al., 2013). In this design, direct fixture points in the silicone mantel are pulled to a central servomotor causing a decrease in volume. In the future, this actuator type shows great promise to be developed and matured into reliable swimming AUVs.

9.5.2.3. Shape memory polymer and dielectric elastomer. The smart material actuators in this section need further work to become efficient in their implementation on the soft robotics field. The SMPs do not use direct current, rather, they use chemicals or magnetic fields as stimuli instead. These alternative stimuli are more difficult to implement into an autonomous AUV design. Although it demonstrates good capabilities as an actuator, there is no previous work of them being used to fabricate AUVs.

DE shows a higher response time and a higher strain than IPMCs but they require a higher voltage to operate. The large amount of strain is produced due to the compliance of the electrodes with the elastomer. There may be a utility in the future for DE as bioinspired systems due to their resemblance to animal muscles based on density, elasticity, pressure, efficiency, and speed, but currently they lack the performance needed.

9.5.2.4. Ionic polymer metallic composites. IPMC actuators are a smart material and have been implemented into robotic systems for their bending and twisting deformation capabilities. To achieve their bending deformations, these actuators use applications of either DC voltage, thermal treatment, light, chemicals, or magnetic fields.

Stimulus through DC voltage to the actuator is the most applicable in AUVs as it is a low voltage input. If the IPMC beam is a free cantilever then the curvature for each cycle of load is not exact as heat stored by the material plays a role in the curvature and return to unbent shape. If the beam is to large, then curling of the IPMC can occur. Theoretically, alternating the polarity on the actuator should cause bending in both directions but due to the thermal capacitance, the flexion will not be symmetric. Yeom and Hu (Yeom and Oh, 2009) found that a heat treatment for these actuators could be beneficial to achieve a better flexion. The IPMC Jellyfish have difficulties with flexion response during activation and relaxation phase. With improvements to this smart material, it could have many more applications in the three classes if the response time between flexion cycles can be reduced.

9.5.2.5. Piezoelectric materials. Piezoelectric material actuators are stimulated by low voltage inputs and are constructed in beam designs like the design of Cen and Erturk (Cen and Erturk, 2013). This actuator offers a moderate power to weight ratio that can perform oscillatory bending vibration. The deformations of these actuators are not large but the work time is dependent on how long power is supplied. Piezoelectric actuators are not as incombered by the heat transfer problem as the IPMC so bending cycles can be induced much more regularly and for longer periods depending on power supply. This type of actuator is not often utilized in AUV design but has possibilities for fluttering fins. In the future, caudal fin designs should incorporate a flexible peduncle shell over the piezoelectric material to help improve bioinspiration.

9.5.2.6. Hydraulic pressure. Robotic systems using fluid actuation show promising capabilities, such as high flexibility, power, and quick response time. Using hydraulic actuators is much more complex since onboard systems are required that will help control them. Such systems will help supply power to the rest of the systems, deliver the fluid throughout the channels, control the fluid's pressure, and control the robot with a communication and control system. All powered systems are stored in a rigid region of the robotic system. The need of all these systems makes soft robots be less efficient than rigid-bodied robots.

Katzschmann et al. (Katzschmann et al., 2016; Katzschmann et al., 2018) recently tested their AUV in a real world oceanic mission for a remote controlled Carangiform AUV. This design had depth control and showed capable forward swimming motion. The next step for this design is to make the system completely autonomous. Clever design could yield AUVs in the Fin Undulation and Jet Propulsion and be an actuator of choice alongside the Cable driven. However, the complex design of the fluidic chambers and their expansion to pressure presents a difficult challenge to overcome.

9.5.2.7. Biohybrid

Biohybrid actuators have shown greater efficiency as they are true biological muscle, and they are the closest approach to mimic biological system. However, since these systems are new, they are still highly experimental, some biohybrid systems lack certain capabilities as turning and maneuvering. The application of ultra-thin membranes (nano-scale thickness) is utilized because it allows for a higher deformation from the muscle contraction. If functioning muscle could be engineered and implemented as a larger actuator, it could change how we look at biorobotics. The biohybrid actuators are the most capable of achieving biomimicry as real muscle is integrated into a polymer-based design. The difficulty for these designs are that they are still in small scale. Large muscle packaging has not been achieved, but with further advances in biomechanics, the possible applications for these actuators could be endless. Advancements in muscular construction for the biohybrid can result in larger designs that are more powerful.

9.6. Materials

The material selection when building an AUV depends greatly on the locomotion and design trying to be achieved. Combination of the materials gives improvements of flexibility for more rigid systems and give soft systems better translated power. However, rigid actuators require a large majority of components to be inflexible, giving the assembly structure strength. The rigid actuators are moving to be more flexible by including flexible joints, more links, and flexible ribs. Peduncle units for multi-link designs are often crafted out of aluminum or rigid plastic, due to their cheapness and machinability. How soft actuators can improve: SMA need to perform higher cycles before failure, IPMC requires improvement in power, SMA and IPMC need to determine the best heat transfer dissipation techniques, and piezoelectric material need to be able to perform larger deformations to produce better thrust. It was found that cable-driven actuators show the best combination crossover between the rigid and soft categories. Hydraulic actuators combine the rigid material protection for the electronic compartment and flexible peduncle to create a capable system. AUVs that utilized propulsive fins had better performance when the fin had some complacency like biological animals.

The electronics compartment for AUVs tend to be rigid encasements that is water tight and made from a plastic. Body shells made of flexible material have become more common as this gives a more mimetic shape (Ichikizaki and Yamamoto, 2007; Shen et al., 2011). These shells can be made from soft or rigid materials that are selected depending on body morphology and shape that is trying to be achieved so the motion is not impeded (Yu et al., 2016b). Soft actuators use elastomers for body coverage because structures need to deform for multiple cycles with low internal resistance, maintain water proofing, and maintain overall shape. Material selection in the future should consider replication of designs for machining and assembly purposes to lower cost and increase number of units produced. In the future, an investigation into the material lifespan of the new combination systems should be conducted.

9.7. Electronics

Electronic selection is a topic all on its own. This review attempts to consolidate and give examples of motors, sensors, and batteries. Another key electrical component would be the control panels that monitor system performance, perform onboard calculations, and output signals depending on programming and construction. Control panels are the device that ties all the other electronics together as they effectively are the brain of the AUV. However, control panels are not included in this review as they require an in depth investigation to help others optimize their robotic systems in the future.

The motors that are used to give mechanical power to rigid or soft actuators are completely dependent on the AUVs needs. The average AUV is small, less than 2 m, so these motors tend to not be large. However, the large AUVs like Yu et al. (Yu et al., 2016b) and Anderson et al. (Anderson and Chhabra, 2002) require a much more powerful DC motor. It is possible to find waterproof actuators which can be submersed.

The best recommendations that can be given at this time is that sensors should be equipped to give the AUV spatial awareness, stability awareness, internal system monitoring, and environmental sampling capabilities. These sensors help the AUV to see obstacles (infrared, cameras, sonar, electrolocation), monitor heading/depth/stability (GPS, inclinometer, attitude transducer, pressure sensor, gyroscope), acceleration/inertia (accelerometer, inertial measurement unit), force/torque (strain gauge, stress sensor), electrical current/water leakage (voltmeter, moisture sensor), temperature/chemical (thermometer/pH sensor). These sensors give the AUV diagnostics about spatial positioning and to take water samples while it swims. This review displays the wide selection of sensors and cameras that can be applied for an array of inputs to help the AUV navigate their environment. These sensors and cameras have been developed into smaller scales and require less power. At the moment, AUVs struggle to perform missions for extended periods of time (Murphy and Haroutunian, 2011). In the future, the motion of these AUVs could be used to power these smaller cameras and sensors by extracting the vibrational motion using energy harvesting techniques (Salazar et al., 2018b).

The batteries give these electronics and the actuators their power but lifespan of these batteries is heavily dependent on usage. Selection of the appropriate battery to maximize swimming capability should be a priority. All the electronics used require a battery that will maintain charge for long periods of time and is rechargeable. That is why Ni-MH, Li-ion, and Li-polymer have been used. Each has advantages and disadvantages and is dependent on the users' needs and budget. The most customizable battery in terms of shape is the Li-polymer, which could be applicable when compact design is required.

10. Conclusions

AUVs are continuing to be optimized to develop an autonomous vehicle so they can be used in real world applications. In efforts to create more optimized AUVs, the kinematic, physical, and hydrodynamic modeling were outlined which lead to the actuator design. The electronics were outlined to show the possibilities for utility and autonomy. The modeling of the biological animals gave a more fundamental understanding of the capabilities and characteristics that gave criteria for the motion and size. Majority of this work expressed the rigid and soft actuators in their respective categories and gave representations of AUVs utilizing these types of actuators. The described AUVs served as a good literature reviews for each category. The more intriguing found AUVs were the ones that include more flexibility for the fin or body actuators. The combination of rigid and soft materials was proposed as biological animals have rigid and soft structures. The selection of materials was assumed to be a top priority to create biomimetic AUVs.

Acknowledgments

The authors, A. Campos and V. Fuentes, gratefully acknowledge the financial support from New Mexico Alliance for Minority Participation. The author, A. Abdelkefi, also acknowledge the financial support from New Mexico Consortium and Los Alamos National Laboratory.

References

Moray Eel Skeleton, Fish, Skull, Taxidermy, Ocean, Reef," WorthPoint Corporation, [Online]. Available: https://www.worthpoint.com/worthopedia/moray-eel-skeleton-fish-skull-taxidermy-ocean. [Accessed 5 2018]..

Tarpon Skeleton," [Online]. Available: https://i.pinimg.com/736x/4d/3e/23/4d3e23595190fb176faddbb304d7b48f.jpg. [Accessed 5 2018].

Abbott, I.H., Doenhoff, A.E.V., 1959. Theory of Wing Sections, Including a Summary of Airfoil Data. Courier Corporation.

Adrian, R.J., 1991. Particle-imaging techniques for experimental fluid mechanics. Annu. Rev. Fluid Mech. 23 (1), 261–304.

Altringham, J.D., Wardl, C.S., I, S.C., 1993. Myotomal muscle function at different locations in the body of a swimming fish. J. Exp. Biol. 182 (1), 191–206.

Anderson, J.M., Chhabra, N.K., 2002. Maneuvering and Stability performance of a robotic tuna. Integr. Comp. Biol. 1, 118–126.

Ansys CFX," ANSYS, Inc., 2018. [Online]. Available: https://www.ansys.com/products/fluids/ansys-cfx. [Accessed 6 6 2018].

Arienti, A., Laschi, C., Giorgio-Serchi, F., Calisti, M., 2015. PoseiDrone Design of a Soft-bodied ROV with Crawling. Swimming and Manipulation Ability. The BioRobotics Institute.

Babu, M.N.P., Mallikarjuna, J.M., Krishnankutty, P., 2016. Hydrodynamic study of freely swimming shark fish propulsion for marine vehicles using 2D particle image velocimetry. Robotics Biomimetics 3 (1), 3.

Bartol, I.K., Patterson, M.R., Mann, R., 2001. Swimming mechanics and behavior of the shallow-water brief squid Lolliguncula brevis. J. Exp. Biol. 204 (21), 3655–3682.

Batchelor, G.K., 2000. An Introduction to Fluid Dynamics. Cambridge University Press.

Behbahani, S.B., Tan, X., 2016. Bio-inspired flexible joints with passive feathering for robotic fish pectoral fins. Bioinspiration Biomimetics 11 (3), 036009.

Behbahani, S.B., Tan, X., 2017. Design and dynamic modeling of electrorheological fluid-based variable-stiffness fin for robotic fish. Smart Mater. Struct. 26, 1–15.

Behl, M., Lendlein, A., 2007. Shape-memory polymers. Mater. Today 10 (4).

Bergmann, M., Lollo, A., 2011. Modeling and simulation of fish-like swimming. J. Comput. Phys. 230, 329–348.

Bhandari, B., Lee, G.Y., Ahn, S.U., 2012. A review on IPMC material as actuators and sensors: fabrications, characteristics and applications. Int. J. Precis. Eng. Manuf. 13 (1), 141–163.

Blevins, E. l., Lauder, G.V., 2012. Rajiform locomotion: three-dimensional kinematics of the pectoral fin surface during swimming in the freshwater stringray Potamotrygon orbignyi. J. Exp. Biol. 215, 3231–3241.

Blindberg, R.D., 2001. The Development of Autonomous Underwater Vehicles (AUV); a Brief Summary. Autonomous Undersea Systems Institute May.

Bonnet, F., Cazenille, L., Seguret, A., Gribovskiy, A., Collignon, B., Halloy, J., Mondada, F., 2017. Design of a modular robotic system that mimics small fish locomotion and body movements for ethological studies. Int. J. Adv. Rob. Syst. 1–12.

Borazjani, I., Sotiropoulos, F., 2008. Numerical investigation of the hydrodynamics of carangiform swimming in the transitional and inertial flow regimes. J. Exp. Biol. 211, 1541–1558.

Borazjani, I., Sotiropoulos, F., 2009. Numerical investigation of the hydrodynamics of anguilliform swimming in the transitional and inertial flow regimes. J. Exp. Biol. 212, 576–592.

Borazjani, I., Sotiropoulos, F., 2010. On the role of form and kinematics of the hydrodynamics of self-propelled body/caudal fin swimming. J. Exp. Biol. 213, 89–107.

Bottom II, R.G., Borazjani, I., Blevins, E.L., Lauder, G.V., 2016. Hydrodynamics of swimming in stingrays: numerical simulations and the role of the leading-edge vortex. J. Fluid Mech. 788, 407–443.

Boxerbaum, A., Shaw, K., Chiel, H., Quinn, R., 2012. Continuous wave peristaltic motion in a robot. Int. J. Robot Res. 302–318.

Buchmann, I., August 2017. What's the Best Battery. Battery University [Online]. Available: http://batteryuniversity.com/learn/archive/whats_the_best_battery 2017.

Cai, Y., Bi, S., Zhang, L., Gao, J., 2009. Design of a robotic fish propelled by oscillating flexible pectoral foils. In: Intelligent Robots and Systems, 2009. IROS 2009. IEEE/RSJ International Conference, pp. 2138–2142.

Castano, M.L., Mavrommati, A., Murphey, T.D., Tan, X., 2017. Trajectory planning and tracking of robotic fish using ergodic exploration. In: American Control Conference.

Cen, L., Erturk, A., 2013. Bio-inspired aquatic robotics by untethered piezohydroelastic actuation. Bioinspiration Biomimetics 8 (1), 016006.

Chen, Z., Shatara, S., Tan, X., 2010. Modeling of biomimetic robotic fish propelled by an ionic polymer-metal composite caudal fin. IEEE/ASME Trans. Mechatron. 15 (3), 448–459.

Chen, Z., Um, T.I., Bart-Smith, H., 2012. Bio-inspired robotic manta ray powered by ionic polymer-metal composite artificial muscles. Int. J. Soc. Netw. Min. 3 (4), 296–308.

Chew, C.M., Lim, Q.Y., Yeo, K.S., 2015. Development of propulsion mechanism for robot manta ray. In: Robotics and Biomimetics (ROBIO). 2015 IEEE International Conference, pp. 1918–1923.

Chu, Z., Zhu, D., 2016. Adaptive sliding mode heading control for autonomous underwater vehicle including actuator dynamics. IEEE Oceans 1–5.

Cianchetti, M., 2013. Fundamentals on the use of shape memory alloys in soft robotics. Interdisciplinary Mechatronics 227–254.

Cianchetti, M., Follador, M., Mazzolai, B., Dario, P., Laschi, C., 2012. Design and development of a soft robotic octopus arm exploiting embodied intelligence. Robot Autom. ICRA IEEE Conf. 5271–5276.

Clapham, R.J., Hu, H., 2014. iSplash-I: high performance swimming motion of a carangiform robotic fish with full-body coordination. In: Robotics and Automation (ICRA), 2014 IEEE International Conference, pp. 322–327.

Colgate, J.E., Lynch, K.M., 2004. Mechanics and control of swimming: a review. IEEE J. Ocean. Eng. 29 (3), 660–673.

Cruz, N., Matos, A., Martins, A., Silva, J., Santos, D., Boutov, D., Pereira, F.L., 1999. Estuarine enviroment studies with Isurus, a REMUS class AUV. In: OCEANS'99 MTS/IEEE. Riding the Crest into the 21st Century, vol. 3. pp. 1205–12010.

Cui, Z., Gu, X., Li, K., Jiang, H., 2017. CFDStudies of the Effects of Waveform on Swimming Performance of Carangifrom Fish. Applied Sciences.

Curet, O.M., Patankar, N.A., Lauder, G.V., Maclver, M.A., 2011. Mechanical properties of a bio-inspired robotic knifish with an undulatory propulsor. Bioinspiration Biomimetics 6 (2), 026004.

Dabiri, J.O., Colin, S.P., Costello, J.H., Gharib, M., 2005. Flow patterns generated by oblate medusan jellyfish: field measurements and laboratory analyses. J. Exp. Biol. 208 (7), 1257–1265.

Daniel, T.L., 1988. Forward flapping flight from flexible fins. Can. J. Zool. 66 (3), 630–638.

Davison, W., 1988. The myotomal muscle of labriform swimming fish is not designed for high speed sustained swimming. NZNS (N. Z. Nat. Sci.) 15, 37–42.

Diazdelcastillo, D., Ly, A., Philips, N., Sinha, A., Wagner, E., 2017. Expedition: Manta Multipurpose Aquatic Navigator and Trash Annihilator," Dissertation.

Fermigier, M., 2017. The use of images in fluid mechanics. Compt. Rendus Mec. 345 (9), 595–604.

Fish, F.E., Schreiber, C.M., Moored, K.W., Liu, G., Dong, H., Bart-Smith, H., 2016. Hydrodynamics performance of aquatic flapping efficiency of underwater flight in the manta. Aerospace 3 (3), 20.

Follador, M., Cianchetti, M., Arienti, a., Laschi, C., 2012. A general method for the design and fabrication of shape memory alloy active spring actuators. Smart Mater. Struct. 21 (11), 115029.

Francis, A., Gupta, V., Mukherjee, S., 2015. An underwater robot mimicking jet propulsion inspired by feather sea star. IEEE 1–7.

Furqan, S., Aasim, T., Zafar, M., Hamza, K., 2017. Hybrid Remotely Operated Underwater Vehicle," Technical Report for the Department of Mechanical Engineering. University of Mumbai.

Gao, J., Bi, S., Xu, Y., Liu, C., 2007. Development and design of a robotic manta ray featuring flexible pectoral fins. In: Robotics and BIomimetics (ROBIO) 2007. IEEE International Conference, pp. 519–523.
Gao, F., Wang, Z., Y, W., Wang, Y., Li, J., 2014. A prototype of a biomimetic mantle jet propeller inspired by cuttelfish actuated by SMA wires and a theorical model for its jet thrust. JBE 11 (3), 412–422.
Gazzola, M., Argentina, M., Mahadevan, L., 2014. Scaling macroscopic aquatic locomotion. Nat. Phys. 10 (10), 758–761.
Gillis, G.B., 1996. Undulatory locomotion in elongate aquatic vertebrates: anguilliform swimming since Sir James Gray. Am. Zool. 36 (6), 656–665.
Gilva, R., Mountoufaris, M., Spyridakis, N., Sfakiotakis, M., 2015. Development of a bio-inspired underwater robot prototype with undeulatory fin propulsion. Proc. NHIBE 15, 81–86.
Giorgio-Serchi, F., Arienti, A., Laschi, C., 2013. Biomimetic Vortex Propulsion: toward the New Paradigm of Soft Unmanned Underwater Vehicles, vol. 18 IEEE/ASME 2.
Giorgio-Serchi, F., Arienti, A., Corucci, F., Giorelli, M., Laschi, C., 2017. Hybrid parameter identification of a multi-modal underwater soft robot. Bioinspiration Biomimetics 12 (2), 025007.
Godaba, H., Li, J., Wang, Y., Zhu, J., 2016. A soft jellyfish robot driven by a dielectric elastomer actuator. IEEE Robot Autom. Lett. 1 (2), 624–631.
Guizzo, E., 2008. Defence contractors snap up submersible robot gliders [update]. IEEE Spectr. 45 (9).
Habib, M.K., 2013. Engineering Creative Design in Robotics and Mechatronics. IGI Global.
High, J.W., Wilkie, W.K., 2003. Method of Fabricating NASA-standard Macro-fiber Composite Piezoelectric Actuators.
Hirata, H., Hayashi, A., Hinayama, Y., Yano, S., Guo, S., 2015. Fluid simulation around tail fin of a fish robot. In: EEE International Conference on Machatronics and Automation. I.
Hove, J.R., O'Bryan, L.M., Gordon, M.S., Webb, P.W., Weihs, D., 2001. Boxfishes (Teleostei: Ostraciidea) as a model system for fishes swimming with many fins: kinematics. J. Exp. Biol. 204 (8), 1459–1471.
Hu, H., Liu, J., Dukes, I., Francis, G., 2006. Design of 3D swim patterns for autonomous robotic fish. In: Intelligent Robots and Systems, 2006 IEEE/RSJ International Conference, pp. 2406–2411.
Hu, T., Shen, L., Lin, L., Xu, H., 2009. Biological inspirations, kinematics modeling, mechanism design and experiments on an undulating robotic fin inspired by Gymnarchus niloticus. Mech. Mach. Theor. 44 (3), 633–645.
Ichikizaki, T., Yamamoto, I., 2007. Development of robotic fish with various swimming. In: Underwater Technology and Workshop on Scientific Us of Submarine Cables and Related Technologies, pp. 378–383.
Jani, J.M., Leary, M., Subic, A., Gibson, M.A., 2014. A review of shape memory alloy research, applications and opportunities. Mater. Des. 56, 1078–1113.
Johnson, W., Soden, P.D., Treman, E.R., 1972. A study in jet propulsion: an analysis of the motion of the squid, Loligo vulgaris. J. Exp. Biol. 56 (1), 155–165.
Kanhere, E., 2017. Bio-inspired Underwater Active and Passive Sensing," Biomimetic Microsensors Inspired by Marine Life. pp. 53–75.
Katzschmann, R.K., Marchese, A.D., Rus, D., 2016. Hydraulic autonomous soft robotic fish for 3D swimming. Exp. Robotic. 405–420.
Katzschmann, R.K., Delpreto, J., MacCurdy, R., Rus, D., 2018. Exploration of underwater life with an acoustically controlled soft robotic fish. Sci. Robotic. 3 (16).
Khalid, M.S.U., Akhtar, I., Dong, H., 2016. Hydrodynamics of tandem fish school with asynchronous undulation of individuals. J. Fluid Struct. 66, 19–35.
Kim, H.S., Lee, J.Y., Chu, W.S., Ahn, S.H., 2016. Design and fabrication of soft morphing ray propulsor: undulator and oscillator. Soft Robot. 00 (00), 1–12.
Koca, G.O., Korkmaz, D., Bal, C., Akpolat, Z.H., Ay, M., 2016. Implementations of the route planning scenarios for the autonomous robotic fish with the optimized propulsion mechanism. Measurement 93, 232–242.
Kodati, P., Kinkle, J., Winn, A., Deng, X., 2008. Microautonomous robotic ostraciiform (MARCO): hydrodynamics, design, and fabrication. IEEE Trans. Robot. 24 (1), 105–117.
Kopman, V., Porfiri, M., 2013. Design, modeling, and characterization of a miniture robotic fish for research and education in biomimetics and bioinspiration. IEEE ASME Trans. Mechatron. 18 (2), 471–483.
Kottapalli, A.G.P., Asadnia, M., 2017. Lateral-line Inspired MEMS Neuromast Sensors," Biomimetic Microsensors Inspired by Marine Life. pp. 1–12.
Krothapalli, A., 1991. The Development of Laser Speckle Velocimetry for the Study of Vortical Flows.
Lachat, D., Crespi, A., Ijspeert, A.J., 2006. Boxybot: a swimming and crawling fish robot controlled by a central pattern generator. In: Biomedical Robotics and Biomechatronics, 2006. BioRob 2006. The First IEEE/RAS-EMBS International Conference, pp. 643–648.
Laschi, C., Cianchetti, M., 2014. Soft Robotics: New Perspectives Fo Robot Bodyware and Control," Frontriers in Bioengineering and Biotechnology.
Laschi, C., Cianchetti, M., Mazzolai, B., Margheri, L., Follador, M., Dario, P., 2012. A soft robot arm inspired by the octopus. Adv. Robot. 26 (7), 709–727.
Laschi, C., Mazzolai, B., Cianchetti, M., 2016. Soft robotics: technologies and systems pushing the boundaries of robot abilites. Sci. Robotic. 1 (1) eaah3690.
Lau, W., Zhong, Y., Du, R., Li, Z., 2015. Bladderless Swaying Wire-driven Robot Shark. IEEE, pp. 155–160.
Lauder, G.V., 2011. Swimming hydrodynamics: ten questions and the technical approaches needed to resolve them. Exp. Fluids 51, 23–35.
Lauder, G.V., 2015. Fish locomotion: recent advances and new directions. Annu. Rev. Mar. Sci. 7, 521–545.
Lauder, G.V., Madden, P., Hunter, I., Tangorra, J., Davidson, N., Proctor, L., Mittal, R., Dong, H., Bozkurttas, M., 2005. Design and performance of a fish fin-like propulsor for AUVs. In: Proceedings of 14th International Symposium on Unmanned Untethered Submersible Technology.
Lauder, G.V., Anderson, E.J., Tangorra, J., Madden, G.A., 2007. Fish biorobotics: kinematics and hydrodynamics of self-propulsion. J. Exp. Biol. 210, 2767–2780.
Lee, Y., Choi, J., Jung, J., Kim, T., Choi, H.T., 2017. Underwater Robot Exploration and Identification Using Dual Imaging Sonar: Basin Test. IEEE Underwater Technology (UT), pp. 1–4.
Li, R., Xiao, Q., Li, L., Liu, H., 2016. Multi-body dynamics modelling on a self-propelled pufferfish with its application in AUV. In: The 10th Symposium on High-performance Marine Vehicles. HIPER.
Liljeback, P., Stravdahl, Ø., Pettersen, K.Y., Gravdahl, J.T., 2014. Mamba - a waterproof snake robot with tactile sensing. In: Intelligent Robots and Systems (IROS 2014), 2014 IEEE/RSJ International Conference, pp. 294–301.
Lin, H.T., Leisk, G.G., Trimmer, B., 2011. GoQBot: a caterpillar-inspired soft-bodied rolling robot. Bioinspiration Biomimetics 6 (2), 026007.
Lin, Y., Kastein, H., Peterson, T., White, C., Lowe, C.G., Clark, C.M., 2013. Using time of flight distance calculations for tagged shark localization witn an AUV. In: Unmanned Untethered Submersible Technology Conference.
Lin, Y., Hsiung, J., Piersall, R., White, C., Lowe, C.G., Clark, C.M., 2016. A multi-autonomous underwater vehicle system for autonomous tracking of marine life. J. Field Robot. 34 (4), 757–774.
Liu, J., Hu, H., 2005. Mimicry of sharp turning behaviours in a robotic fish. In: Robotics and Automotion (ICRA 2005, pp. 3318–3323.
Liu, J., Hu, H., 2010. Biological inspiration: from carangiform fish to multi-joint robotic fish. JBE 7 (1), 35–48.
Liu, J., Dukes, I., Hu, H., 2005. Novel mechatronics design for a robotic fish. In: Intelligent Robots and Systems, 2005. (IROS 2005). 2005 IEEE/RSJ International Conference, pp. 807–812.
Liu, F., Lee, K.M., Yang, C.J., 2012. Hydrodynamics of an undulating fin for a wave-like locomotion system design. IEEE ASME Trans. Mechatron. 17 (3), 554–562.
Liu, G., Ren, Y., Zhu, J., Bart-Smith, H., Dong, H., 2015. Thrust producing mechanisms in ray-inspired underwater vehicle propulsion. Theor. Appl. Mech. Lett. 5, 54–57.
Liu, H., Taylor, B., Curet, O.M., 2017. Fin ray stiffness and fin morphology control ribbon-fin-based propulsion. Soft Robot. 4 (2), 103–116.
Low, K.H., Willy, A., 2005. Development and initial investigation of NTU robotic fish with modular flexible fins. In: Mechatronics and Automation, 2005 IEEE International Conference, vol. 2. pp. 958–963.
Low, K.H., Zhou, C., Seet, G., Bi, S., Cai, Y., 2011. Improvement and testing of a robotic manta ray (RoMan-III). In: Robotics and Biomimetics (ROBIO). 2011 IEEE International Conference, pp. 1730–1735.
Ltd, T.O.F., 2011-2018. OpenFoam," the OpenFOAM Foundation Ltd. [Online]. Available: https://openfoam.org, Accessed date: 6 June 2018.
Mainong, A., Acob, A., Archad, M., 2017. Investigating pectoral shapes and locomotive strategies for conceptual designing bio-inspired robotic fish. J. Eng. Sci. Technol. 12 (1), 1–14.
Manfredi, L., Assaf, T., Mintchev, S., Marrazza, S., Capantini, L., Orofino, S., Ascari, L., Grillner, S., Wallen, P., Okeberg, O., Stefanini, C., Dario, P., 2013. A Bioinspired autonomous swimming robot as a tool for studying goal-directed locomotion. Biol. Cybern. 107 (5), 513–527.
Marchese, A., Onal, C., Rus, D., 2014. Autonomous soft robotic fish capable of escape maneuvers using fluidic elastomer actuators. Soft Robot. 1 (1).
Marchese, A., Katzschmann, R.K., Rus, D., 2015. A recipe for soft fluidic elastomer robots. Soft Robot. 2 (1).
Marras, S., Porfiri, M., 2012. Fish and robots swimming together: attraction towards the robot demands biomimetic locomotion. J. R. Soc. Interface. https://doi.org/10.1098/rsif.2012.0084.
Mason, R., Burdick, J.W., 2000. Experiments in carangiform robotic fish locomotion. In: IEEE International Conference on Robotics & Automation.
McHenry, M.J., Jed, J., 2003. The ontogentic scaling of hydrodynamics and swimming performance in jellyfish (Aurelia aurita). J. Exp. Biol. 206, 4125–4137.
Mirfakhrai, T., Wadden, J., Baughman, R.H., 2007. Polymer artificial muscles. Mater. Today 10 (4), 30–38.
K. W. Moored and H. Bart-Smith, Hydrodynamic Performance of a Manta Ray Inpsired Oscillating Fin, Univeristy of Virginia, Department of Mechanical and Aerospace Engineering.
Munasinghe, K., Aseeri, M., Almorqi, S., Hossain, M.F., Wali, M.B., Jamalipour, A., 2017. EM-based high speed wireless sensor networks for underwater surveillance and target tracking. J. Sens. 1–14.
Munson, B.R., Okiishi, T.H., Huebsch, W.W., Rothmayer, A.P., 2013. Fundamentals of Fluid Mechanics. John Wiley Sons, Inc.
Murphy, A.J., Haroutunian, M., 2011. Using bio-inspiration to improve capabilities of underwater vehicles. In: 17th International Unmanned Untethered Submersible Technology Conference.
Najem, J., Sarles, S.A., Akle, B., Leo, D.J., 2012. Biomimetic jellyfish-inspired underwater vehicle actuated by ionic polymer metal composite actuators. Smart Mater. Struct. 21 (9), 094026.
Nawroth, J.C., Lee, H., Feinberg, A.W., Ripplinger, C.M., McCain, M.L., Grosberg, A., Parker, K.K., 2012. A tissue-engineered jellyfish with biomimetic propulsion. Nat. Biotechnol. 30 (8), 792–797.
Nelson, K., Mohseni, K., 2017. An artificial fish lateral line sensory system composed of modular pressure sensor blocks. In: IEEE International Conference on Robotics and Automation.
Neveln, I.D., Bai, Y., Snyder, J.B., Solberg, J.R., Curet, O.M., Lynch, K.M., MacIver, M.A., 2013. Biomimetic and bio-inspired robotics in electric fish research. J. Exp. Biol. 216 (3), 2501–2514.
Nir, S., Shraga, S., Moshe, B.B., Ruchaevski, I., Shteinberg, T., 2012. A Jellyfish like Robot

Mimicking Jet Propulsion. IEEE.
Niu, C., Zhang, L., Bi, S., Cai, Y., 2012. Development and depth control of a robotic fish mimicking cownose ray. In: Robotics and Biomimetics (ROBIO), 2012 IEEE International Conference, pp. 814–818.
Onal, C.D., Chen, X., Whitesides, G.M., Rus, D., 2017. Soft mobile robots with on-board chemical pressure generation. In: Robotics Research. Springer, Cham, pp. 525–540.
Park, S.J., Gazzola, M., Park, K.S., Di Santo, V., Blevins, E.L., Pasqualini, F.S., 2016. Phototactic guidance of a tissue-engineered soft-robotic ray. Science 353 (6295), 158–162.
Pelrine, R., Kornbluh, R., Pei, Q., Stanford, S., Oh, S., Eckerle, J., Full, R., Rosenthal, M., Meijer, K., 2002a. Dielectric elastomer artificial muscle actuators: toward biomimetic motion. In: Smart Structures and Materials 2002: Electroactive Polymer Actuators and Devices (EAPAD), vol. 4695. pp. 126–137.
Pelrine, R., Kornbluh, R., Pei, Q., Stanford, S., Oh, S., Eckerle, J., 2002b. Dielectric elastomer artificial muscle actuators: toward biomimetic motion. Proc. SPIE 4695, 126–137.
Pinterest, "Tuna skeleton," [Online]. Available: http://www.fishingfury.com/wp-content/uploads/2008/06/blue-runner-skeleton.jpg.
Pollard, B., Tallapragada, P., 2017. An aquatic robot propelled by an internal rotor. IEEE ASME Trans. Mechatron. 22 (2), 931–939.
Prats, F.R., 2015. Hydrodynamics of Pitching Foils: Flexibility and Ground Effects.
Punning, A., Anton, M., Kruusmaa, M., Aabloo, A., 2004. A biologically inspired ray-like underwater robot with elctroactive polymer pectoral fins. In: International IEEE Conference on Mechatronics and Robotics, pp. 241–245.
Pyo, J., Song, S., Yu, S.C., 2017. Acoustic Beam-based Man-made Underwter Landmark Detection Method for Multi-beam Sonar. IEEE Underwater Technology (UT), pp. 1–5.
Raj, A., Thakur, A., 2016. Fish-inspired robots: design, sensing, actuation, and autonomy-A review of research. Bioinspiration Biomimetics 11 (3), 031001.
Ramamurti, R., Sandberg, W.C., Lohner, R., Walker, J.A., Westneat, M.W., 2002. Fluid dynamics of flapping aquatic flight in the bird wrasse: three-dimensional unsteady computations with fin deformation. Exp. Biol. 205, 2997–3008.
Ravalli, A., Rossi, C., Marrazza, G., 2017. Bio-inspired fish robot based on chemical sensors. Sensor. Actuator. B Chem. 239, 325–329.
Ren, Z., Yang, X., Wang, T., Wen, L., 2015. Hydrondynamics of a robotic fish tail: effects of the caudal peduncle fin ray motions and the flow speed. Bioinspiration Biomimetics 11 (1) 01608.
Rico, J.A.S., Endo, G., Hirose, S., Yamada, H., 2017. Development of an actuation system based on water jet propulsion for a slim long-reach robot. ROBOMECH J. 4 (8).
Ricotti, L., Fujie, T., 2017. Thin polymeric films for building biohybrid microbots. Bioinspiration Biomimetics 12 (2), 021001.
Ricotti, L., Menciassi, A., 2012. Bio-hybrid muscle cell-based actuators. Biomed. Microdevices 14 (6), 987–998.
Rollinson, D., Bilgen, Y., Brown, B., Enner, F., Ford, S., Layton, C., Rembisz, J., Schwerin, M., Willig, A., Velagapudi, P., Choset, H., 2014. Design and architecture of a series eleastic snake robot. In: Intelligent Robots and Systems (IROS 2014), 2014 IEEE RSJ International Conference, pp. 4630–4636.
Salazar, R., Fuentes, V., Abdelkefi, A., 2018a. Classification of biological and bioinspired aquatic systems: a review. Ocean Eng. 148, 75–114.
Salazar, R., Taylor, G., Khalid, M.S.U., Abdelkefi, A., 2018b. Optimal design and energy harvesting performance of carangiform fish-like robotic system. Smart Mater. Struct. 27, 075045.
Scaradozzi, D., Palmieri, G., Costa, D., Pinelli, A., 2017a. BCF scimming locomotion for autonomous underwater robots: a review and a novel solution to improve control and efficiency. Ocean Eng. 130, 437–453.
Scaradozzi, D., Palmieri, G., Costa, D., Zingaretti, S., Panebianco, L., Ciuccoli, N., Pinelli, A., Callegari, M., 2017b. UNIVPM BRAVe: a hybrid propulsion underwater research vehicle. Int. J. Autom. Technol. 11 (3), 404–414.
Schosser, C., Fuchs, T., Hain, R., Kahler, C. j., 2016. Non-intrusice calibration for three-dimensional particl imaging. J. Exp. Fluids 57 (5), 69.
Seok, S., Onal, C.D., Cho, K.J., Wood, R.J., Rus, D., Kim, S., 2013. Meshworm: a peristaltic soft robot with antagonistic nickel titanium coil actuators. IEEE ASME Trans. Mechatron. 18 (5), 1485–1497.
Seok, S., et al., 2010. Peristaltic locomotion with antagonistic actuators in soft robotics. In: 2010 IEEE International Conference on Robotics and Automation, pp. 1228–1233.
Sfakiotakis, M., Fasoulas, J., 2014. Development and experimental validation of a model for the memvrane restoring torques in undulatory fin mechanisms. In: 22nd Mediterranean Conference on Control and Automative (MED).
Sfakiotakis, M., Lane, D.M., Davies, J.B.C., 1999. Review of FIsh swimming modes for aquatic locomotion. IEEE J. Ocean. Eng. 24 (2), 237–252.
Shang, L., Wang, S., Tan, M., Cheng, L., 2012. Swimming locomotion modeling for biomimetic underwater vehicle with two undulating long-fins. Robotica 30, 913–923.
Shen, F., Wei, C., Cao, Z., Xu, D., Yu, J., Zhou, C., 2011. Implementation of a multi-link robotic dolphin with two 3-DOF flippers. J. Comput. Inf. Syst. 7 (7), 2601–2607.
Shen, Q., Wang, T., Kim, K.J., 2015. A biomimetic underwater vehicle actuated by waves with ionic polymer-metal composite soft sensors. Bioinspiration Biomimetics 10 (5), 055007.
Shoele, K., Zhu, Q., 2010. Numerical simulation of a pectoral fin during labriform swimming. J. Exp. Biol. 213, 2038–2047.
Siahmansouri, M., Ghanbari, A., Fakhrabadi, M.M.S., 2011. Design, implementation and control of a fish robot with undulating fins. Int. J. Adv. Rob. Syst. 8 (5), 60.
Sitorus, P.E., Nazaruddin, Y.Y., Leksono, E., Budiyono, A., 2009. Design and impementation of pared pectoral fins locomotion of labriform fish applied to a fish robot. JBE 6 (1), 37–45.
Smith, C., Villanueva, A., Joshi, K., Tadesse, Y., Priya, S., 2010. Working principle of bio-inspired shape memory alloy composite actuators. Smart Mater. Struct. 20 (1), 012001.
Solberg, J.R., Lynch, K.M., MacIver, M.A., 2008. Active electrolocation for underwater target localization. Int. J. Robot Res. 27 (5), 529–548.
Sprinkle, B., Bale, R., Bhalla, A.P.S., MacIver, M.A., Patankar, N.A., 2017. Hydrodynamic Optimality of balistiform and gymnotiform locomotion. Eur. J. Comput. Mech. 1–13.
Stefanini, C., Orofino, S., Manfredi, L., Mintchev, S., Marrazza, S., Assaf, T., Sinibaldi, E., Grillner, S., Wallen, P., Dario, P., 2012. A compliant bioinspired swimming robot with nero-inspired control and autonomous behavior. In: Robotics and Automation (ICRA), 2012 IEEE International Conference, pp. 5094–5098.
Studebaker, E., Ermlick, W., Warner, R., Hart, B., Pandey, A., Smith, H., Sienkiewiez, L., Baillargeon, J., Roberson, N., An, J., Gater, B., Feaster, J., Jung, S., Bayandor, J., 2016. Bio-inspired Robotic Undulatory Stingray," ASME 2016 Fluids Engineering Division Summer Meeting.
Su, Z., Yu, J., Tan, M., Zhang, J., 2014. Implementing flexible and fast turning maneuvers of a multijoint robotic fish. IEEE ASME Trans. Mechatron. 19 (1), 329–338.
Suebsaiprom, P., Lin, C., Engkaninan, A., 2016. Undulatory locomotion and effective propulsion for fish-inspired robot. Contr. Eng. Pract. 58, 66–77.
Takagi, K., Yamamura, M., Luo, Z.W., Onishi, M., Hirano, S., Asaka, K., Hayakawa, Y., 2006. Development of a rajiform swimming robot using ionic polymer artificial muscles. In: Intelligent Robots and Systems, 2006 IEEE/RSJ International Conference, pp. 1861–1866.
Tan, X., 2011. Autonomous robotic fish as mobile sensor platforms: challenges and potential solutions. Mar. Technol. Soc. J. 45 (4), 31–40.
Techet, A.H., Hover, F.S., Triantafyllou, M.S., 2004. Separation and turbulence control in biomimetic flows. Flow, Turbul. Combust. 71, 105–118.
Tolkoff, S.W., 1999. Robotics and Power Measurments of the RoboTuna. Doctoral Dissertation Massachusetts Institute of Technology.
Trabia, S., Palmre, V., Kim, K.J., 2015. Development of self-sensing Ionic Polymer-Metal Composite soft robotic actuator integrated with gallium-indium alloy. Ubiquitous Robot. Ambient Intell.(URAI) 368–369.
Trabia, S., Shen, Q., Stalbaum, T., Hunt, R., Hwang, T., Kim, K., 2016. Numerical and Experimental Investigation of a Biomimetic Robotic Jellyfish Actuated by Ionic Polymer-metal Composite," Ubiquitous Robots and Ambient Intelligence. pp. 204–205.
Trimmer, B., Laschi, C., Kim, S., 2013. Soft robotics: a bioinspired evolution in robotics. Trends Biotechnol. 31 (5), 287–294.
Trivedi, D., Rahn, C.D., Kier, W.M., Walker, I., 2008. Soft robotics: biological inspiration, state of art, and future research. Appl. Bionics Biomechanics 5 (3), 99–117.
Tytell, E.D., 2004. The hydrodynamics of eel swimming II. Effect of swimming speed. J. Exp. Biol. 207, 3265–3279.
Umedachi, T., Vikas, V., Trimmer, B.A., 2016. Softworms: the design and control of non-pneumatic, 3D-printed, deformable robots. Bioinspiration Biomimetics 11 (2), 025001.
Vasudev, K.L., Sharma, R., Bhattacharyya, S.K., 2014. A multi-objective optimization design framework integrated with CFD for the design of AUVs. Meth. Oceanogr. 10, 138–165.
Videler, J.J., Steele, J., Thorpe, S., Thurekian, K., 2001. Fish locomotion. Encycl. Ocean Sci. 938–946.
Villanueva, A.A., Joshi, K.B., Blottman, J.B., Priya, S., 2010. A bio-inspired shape memory alloy composite (BISMAC) actuator. Smart Mater. Struct. 19 (2), 025013.
VIllanueva, A., Smith, C., Priya, S., 2013. A Biomimetic Robotic Jellyfish (Robojelly) Actuated by Shape Memory Alloy Composite Actuators. Bioinspiration & Biomimetics.
Walker, J.A., Westneat, M.W., 1997. Labriform propulsion in fishes: kinematics of flapping aquatic flight in the bird wrasse Gomphosus varius (Labridae). J. Exp. Biol. 200, 1549–1569.
Walker, J.A., Westneat, M.W., 2002. Kinematics, dynamics, and energetics of rowing and flapping propulsion in fishes. Integr. Comp. Biol. 1032–1043.
Wang, W., Xie, G., 2014. CPG-based locomotion controller design for a boxfish-like robot. Int. J. Adv. Rob. Syst. 11 (6), 87.
Wang, Y., Wang, Z., Li, J., 2011. Initial design of a biomimetic cuttlefish robot actuated by SMA wires. In: Measuring Technology and Mechatronics Automation (ICMTMA), vol. 2. pp. 425–428.
Wang, W., Guo, J., Wang, Z., Xie, G., 2013. Neural controller for swimming modes and gait transition on an ostraciiform fish robot. In: Advanced Intelligent Mechatronics (AIM), 2013 IEEE/ASME International Conference, pp. 1564–1569.
Wang, W., Xie, G., Shi, H., 2014. Dynamic modeling of an ostraciiform robotic fish based on angle of attack theory. In: International Joint Conference on Neral Networks, Beijing, China.
Wang, W., Gu, D., Xie, G., 2017a. Autonomous optimization of swimming gait in a fish robot with multiple onboard sensors. IEEE Trans. Syst Man Cybern.: Syst. (99), 1–13.
Wang, S., Wang, Y., Wei, Q., Tan, M., Yu, J., 2017b. A bio-inspired robot with undulatory fins and its control methods. IEEE/ASME Trans. Mechatron. 22 (1), 206–216.
Wang, W., Liu, J., Xie, G., Wen, L., Zhang, J., 2017c. A bio-inspired electrocommunication system for small underwater robots. Bioinspiration Biomimetics 1 (3), 036002.
Wang, Z., Wang, Y., Li, J., Hang, G., 2009. A micro biomimetic manta ray robot fish actuated by SMA. In: Robotics and Biomimetics (ROBIO). 2009 IEEE International Conference, pp. 1809–1813.
Wardle, C.S., Videler, J.J., 1980. Aspects of Animal Movement,Fish Swimming," Aspects of Animal Movement. Cambridge University Press, pp. 125–150.
Webb, P.W., Weihs, D., 2015. Stability versus maneuvering: challenges for stability during swimming by fishes. Integr. Comp. Biol. 55 (4), 753–764.
Wen, L., Lauder, G., 2013. Understanding undulatory locomotion in fishes using an inertia-compensated flapping foil robotic device. Bioinspiration Biomimetics 8 (4), 046013.
Wen, L., Wang, T., Wu, G., Liang, J., Wang, C., 2012. Novel method for the modeling and control investigation of efficient swimming for robotic fish. IEEE Trans. Ind. Electron.

59 (8).
Westerweel, J., 1997. Fundamentals of digital particle image velocimetry. Meas. Sci. Technol. 8 (12), 1379.
Westneat, M.W., 1996. Functional morphology of aquatic flight in fishes: kinematics, electromyography, and mechanical modeling of labriform locomotion. Am. Zool. 36 (6), 582–598.
Wettergreen, D., Gaskett, C., Zelinsky, A., 1998. Development of a visually-guided autonomous underwater vehicle. OCEANS'98 Conf. Proc. 2, 1200–1204.
Weymouth, G.D., Subramaniam, V., Triantafyllou, M.S., 2015. Ultra-fast escape maneuver of an octopus-inspired robot. Bioinspiration Biomimetics 10 (1), 016016.
Wu, T.Y.T., 1961. Simming of a waving plate. J. Fluid Mech. 10 (3), 321–344.
Wu, Z., Yu, J., Yuam, J., Tan, M., Zhang, J., 2015. Mechatronic design and implementation of a novel gliding robotic dolphin. Robotic. Biomimetics (ROBIO) 267–272.
Wu, Z., Liu, J., Yu, J., Fang, H., 2017. Development of a Novel Robotic Dolphin and its Application to Water Quality Monitoring. IEEE/ASME Transactions on Mechatronics.
Xiang, C., Yang, H., Sun, Z., Xue, B., Hao, L., Rahoman, M.A., Davis, S., 2017. The design, hysteresis modeling and control of a novel SMA-fishing-line actuator. Smart Mater. Struct. 26 (3), 037004.
Xie, H., Zhou, H., Shen, L., Yin, D., 2016. Mechanism design, dynamics modelling and experiments of bionic undulating fins. Int. J. Robot Autom. 31 (2).
Xiong, G., Lauder, G.V., 2013. Center of mass motion in swimming fish: effects of speed and locomotor mode during undulatory propulsion. Zoology 117 (4), 269–281.
y Alvarado, P.V., Chin, S., Larson, W., Mazumbar, A., Youcef-Toumi, K., 2013. A soft body under-actuated approach to multi degree of freedom biomimetic robots: a stingray example. In: Biomedical Robotics and Biomechatronics (BioRob), 2013 3rd IEEE RAS and EMBS International Conference, pp. 473–478.
Yamamoto, I., 2017. Robotic fish development for the next generation underwater vehicle. Adv. Sci. Technol. 101, 95–103.
Yang, S.B., Qui, J., Han, X.Y., 2009. Kinematics modeling and experiments of pectoral oscillation propulsion robotic fish. J. Bionic Eng. 6 (2), 174–179.
Yen, T., Azwadi, C.N., 2015. A review: the development of flapping hydrodynamics of body and caudal fin movement fishlike structure. J. Adv. Rev. Sci. Res. 1 (19), 8–38.
Yeom, S.W., Oh, I.K., 2009. A biomimetic jellyfish robot based on ionic polymer metal composite actuators. Smart Mater. Struct. 18 (8), 085002.
Youngerman, E.D., Flammang, B.E., Lauder, G.V., 2014. Locomotion of free-swimming ghost knifefish: anal fin kinematics during four behaviours. Zoology 117 (5), 337–348.
Yu, J., Wei, C., 2013. Towards development of a slider-crank centered self-propelled dolphin robot. Adv. Robot. 27 (12), 971–977.
Yu, J., Tan, M., Wang, S., Chen, E., 2004. Development of a biomimetic robotic fish and its control algorithm. IEEE Trans. Syst. Man Cybern. Part B (Cybernetics) 34 (4), 1798–1810.
Yu, S., Ma, S., Li, B., Wang, Y., 2009. An ammphibious snake-like robot: design and motion experiments on ground and in water. In: Information and Automation, 2009. ICIA '09. International Conference, pp. 500–505.
Yu, J., Ding, R., Yang, Q., Tan, M., Wang, W., Zhang, J., 2012. On a bio-inspired amphibious robot capble of multimodal motion. IEEE ASME Trans. Mechatron. 17 (5), 847–856.
Yu, J., Wang, K., Tan, M., Zhang, J., 2014. Design and control of an embedded vision guided robotic fish with multiple control surfaces. Sci. World J. 2014, 631296.
Yu, J., Zhang, C., Liu, L., 2016a. Design and control of a single-motor-actuated robotic fish capable of fast swimming and maneuverability. IEEE ASME Trans. Mechatron. 21 (3), 1711–1719.
Yu, J., Su, Z., Wu, Z., Tan, M., 2016b. Development of a fast-swimming dolphin robot capable of leaping. IEEE ASME Trans. Mechatron. 21 (5), 2307–2316.
Zhang, K., Sun, Q., 2017. Cyclic compressive responses of NiTI shape memory allowy-effects of loading frequency. Adv. Shape Memory Metal: Adv. Struct. Mater. 73, 231–241.
Zhang, S., Qian, Y., Liao, P., Qin, F., Yang, J., 2016. Design and control of an agile robotic fish with integrative biomimetic mechanism. IEEE ASME Trans. Mechatron. 21 (4), 1846–1857.
Zheng, L., Bi, S., Cai, Y., Niu, C., 2010. Design and optimization of a robotic fish mimicking cow-nosed ray. In: IEEE, International Conference on Robotics and Biomimetics, pp. 1075–1080 December.
Zhong, Y., Li, Z., Du, R., 2017. A Novel Robot Fish with Wire-driven Active Body and Complaint Tail. IEEE/ASME Transactions on Mechatronics.
Zhou, C., Low, K.H., 2012. Design and locomotion control of a biomimetic underwater vehicle with fin propulsion. IEEE ASME Trans. Mechatron. 17 (1), 25–35.
Zhou, P., Liu, T., Zhou, X., Mou, J., Zheng, S., Gu, Y., Wu, D., 2017. Overview of progress in development of the bionic underwater propulsion system. J. Biomimetics Biomater. Biomed. Eng. 32, 9–19.